Interactions between Fe and organic matter and their impact on As(V) and P(V)

Anneli Sundman

Department of Chemistry

Umeå, 2014

Cover photo: Anneli Hellström, 1996

ISBN: 978-91-7601-020-4

Electronic version available at http://umu.diva-portal.org/

Printed by: Service Center KBC

Umeå, Sweden 2014

To my family.

Table of contents

Abstract iii

Abbreviations iv

List of papers v

Populärvetenskaplig sammanfattning på svenska vii

1. Introduction 1

1.1 Natural organic matter 2

1.2 Fe speciation in natural systems 2

1.3 Arsenic 3

1.4 Phosphorous 5

1.5 XAS 5

1.6 Krycklan Catchment 7

2. Outline of this thesis 9

3. Materials and Methods 10

3.1 Chemicals, solutions and pH measurements 10

3.2 Thermodynamic calculations 11

3.3 Preconcentration protocol 11

3.3.1 Characterization of preconcentration protocol 13

3.4 Collection and preparation of samples from the Krycklan Catchment 14

3.5 Preparation of As(V)/P(V)-Fe(III)-NOM samples 15

3.6 Collection and analysis of XAS data 16

3.6.1 XANES and pre-edge analysis 16

3.6.2 Wavelet transform 17

3.6.3 EXAFS 18

3.7 Infrared spectroscopy 19

4. Results and Discussion 20

4.1 Evaluation of preconcentration protocol 20

4.2 Fe speciation in the Krycklan Catchment 23

4.2.1 Fe speciation in C2 stream water 25
4.2.2 Effect of surrounding landscape 31
4.2.3 Iron speciation within adjacent landscape elements 33
4.2.4 Reactivity of Fe from a natural stream water towards As(V) 39
4.3 Studies of ternary As(V)/P(V)-Fe(III)-NOM systems 43
4.3.1 Binary Fe(III)-NOM systems 43
4.3.2 IR spectroscopic results in the ternary systems 44
4.3.3 XANES and WT analysis of the ternary systems 46
4.3.4 EXAFS results for the ternary systems 50
5. Summary and future work 52
5.1 Possibilities with the preconcentration protocol 53
5.2 Fe speciation in Krycklan Catchment 53
5.2.1 Geochemical significance of Fe(II, III)-NOM complexes 53
5.2.2 Implications of Fe speciation in the Krycklan catchment 54
5.3 The ternary As(V)/P(V)-Fe(III)-NOM systems 55
5.3.1 Properties of Fe(III)-NOM complexes 55
5.3.2 The identity of As(V)/P(V) bearing Fe phases 56
6. Acknowledgement 58
7. References 60

Abstract

Iron (Fe) speciation is important for many biogeochemical processes. The high abundance and limited solubility of Fe(III) are responsible for the widespread occurrence of Fe(III) minerals in the environment. Co-precipitation and adsorption onto mineral surfaces limits the free concentrations of compounds such as arsenate (As(V)), Fe(III) and, phosphate (P(V)). Mineral dissolution, on the other hand, might lead to elevated concentrations of these compounds. Fe speciation is strongly affected by natural organic matter (NOM), which suppresses hydrolysis of Fe(III) via complexation. It limits the formation of Fe(III) minerals and Fe(III) co-precipitation. This thesis is focused on interactions between Fe(III) and NOM as well as their impact on other elements (i.e. As(V) and P(V)). X-ray absorption spectroscopy (XAS) was used to obtain molecular scale information on Fe and As speciation. This was complemented with infrared spectroscopy, as well as traditional wet-chemical analysis, such as pH and total concentration determinations. Natural stream waters, soil solutions, ground water and soil samples from the Krycklan Catchment, in northern Sweden, were analyzed together with model compounds with different types of NOM. A protocol based on ion exchange resins was developed to concentrate Fe from dilute natural waters prior to XAS measurements. Iron speciation varied between the stream waters and was strongly affected by the surrounding landscape. Stream waters originating from forested or mixed sites contained both Fe(II, III)-NOM complexes and precipitated Fe(III) (hydr)oxides. The distribution between these two pools was influenced by pH, total concentrations and, properties of NOM. In contrast, stream waters from wetland sites and soil solutions from a forested site only contained organically complexed Fe. Furthermore, the soil solutions contained a significant fraction Fe(II)-NOM complexes. The soil samples were dominated by organically complexed Fe and a biotite-like phase. Two pools of Fe were also identified in the ternary systems with As(V) or P(V) mixed with Fe(III) and NOM: all Fe(III) was complexed with NOM at low total concentrations of Fe(III), As(V) and/or P(V). Hence, Fe(III) complexation by NOM reduced Fe(III)-As(V)/P(V) interactions at low Fe(III) concentrations, which led to higher bioavailability. Exceeding the Fe(III)-NOM complex equilibrium resulted in the occurrence of Fe(III)-As(V)/P(V) (co-)precipitates.

Abbreviations

CN	Coordination Number
DMEA	DiMetylEthanol Amine
DOC	Dissolved Organic Carbon
EXAFS	Extended X-Ray Absorption Fine Structure
FA	Fulvic Acid
FT	Fourier Transform
HA	Humic Acid
IR	InfraRed
LCF	Linear Combination Fitting
NOM	Natural Organic Matter
PPHA	Pahokee Peat Humic Acid
R	Bond distance
SRFA	Suwannee River Fulvic Acid
SRN	Suwannee River Natural Organic Matter
SSRL	Stanford Synchrotron Radiation Lightsource
TMA	TriMethyl Amine
TOC	Total Organic Carbon
WT	Wavelet Transform
XANES	X-ray Absorption Near Edge Structure
XAS	X-ray Absorption Spectroscopy

List of papers

This thesis is based on the following papers, which are referred to in the text by their Roman numerals, I-V.

I. An experimental protocol for structural characterization of Fe in dilute natural waters

Sundman A., Karlsson T., Persson P.

II. XAS study of iron speciation in soils and waters from a boreal catchment

Sundman A., Karlsson T., Laudon H., Persson P.

III. Reactivity of Fe from a natural stream water towards As(V)

Sundman A., Karlsson T., Persson P.

Manuscript prepared for submission to Applied Geochemistry

IV. Complexation and precipitation reactions in the ternary As(V)-Fe(III)-NOM (natural organic matter) system

Sundman A., Karlsson T., Sjöberg S., Persson P.

Manuscript prepared for submission to Geochimica et Cosmochimica Acta

V. Complexation and precipitation reactions in the ternary P(V)-Fe(III)-NOM (natural organic matter) system

Sundman A., Karlsson T., Sjöberg S., Persson P.

Manuscript

Author's contributions

For all papers, I-V, the work conducted at Stanford Synchrotron Lightsource (SSRL), i.e. collection of X-ray absorption spectroscopy (XAS) spectra, was shared between A. Sundman, K. Hagvall, T. Karlsson and P. Persson.

Paper I: A. Sundman co-designed and conducted the experiments, collected the majority of the XAS spectra, did the majority of the data reduction/evaluation and was the main author.

Paper II: A. Sundman co-designed and conducted the experiments, collected some of the XAS spectra, did the majority of the data reduction/evaluation and was the main author.

Paper III: A. Sundman designed and conducted the experiments, did substantial data reduction/evaluation and was the main author.

Paper IV: A. Sundman co-designed the project, prepared and measured all IR spectroscopy samples, prepared a few XAS samples, collected some XAS spectra, did substantial data reduction/evaluation on the IR and XAS data, assisted with input data for the thermodynamic calculations and was the main author.

Paper V: A. Sundman co-designed the project, prepared and measured the majority of the IR spectroscopy and XAS samples, did substantial data reduction/evaluation of the IR and XAS data and was the main author.

Populärvetenskaplig sammanfattning på svenska

Järn (Fe) är ett av de vanligast förekommande grundämnena. Det återfinns bland annat i de röda blodkropparna, i levern, i olika enzym/protein, samt i jordskorpan. Järn kan förekomma i många olika former och föreningar, men i jordskorpan återfinns järn främst i form av olika järnmineraler. Järnmineralerna kännetecknas av att de har olika kristallinitet, det vill säga olika ordnade strukturer, olika sammansättningar, samt ofta väldigt stora ytareor. Dessa ytareor är en av anledningarna till varför järnet spelar en så stor roll för många andra ämnen i naturen, t.ex. näringsämnen som fosfor eller gifter som arsenik och kvicksilver. I naturliga system spelar även nedbrytningsprodukter från växter och djur, det vill säga organiskt material, en viktig roll. Dessa påverkar storleken på järnmineral-partiklarna och det organiska materialet kan också bilda stabila föreningar/komplex med järnet så att bildningen av järnmineraler förhindras. Detta medför att järnet blir mer biotillgängligt, det vill säga åtkomligt för mikroorganismer och växter. Järn kan även reglera de fria halterna av näringsämnen eller gifter, t.ex. fosfor och arsenik, genom bildning av nya fasta järninnehållande faser. Det är styrkan på föreningen mellan järn och organiskt material som avgör hurvida järnet förblir lösligt eller bildar en fast fas. Järn spelar också en viktig roll genom att vara ett redoxaktivt ämne, d.v.s. ett ämne som kan avge eller ta upp elektroner. Dessa reaktioner kan vara beroende av tillgång till syre, solljus eller mikroorganismer och påverkar både kol- och kvävecyklerna i naturen.

Den här avhandlingen består av fem delarbeten som alla fokuserar på interaktioner mellan järnkomplex i vattenlösning och organiskt material. I de två första arbetena har järnföreningar (t.ex. järnmineraler eller olika typer av järnjoner) i bäckar, marklösningar, grundvatten och jordprover från ett välkarakteriserat borealt avrinningsområde i norra Sverige studerats för att bättre förstå vilka former av järn som förekommer, hur de påverkas av den omgivande miljön och hur järnet transporteras inom närliggande områden. I det tredje arbetet tillsattes arsenat (den vanligaste formen av arsenik i syrerika naturliga miljöer) till naturligt bäckvatten, från samma avrinningsområde, för att dels undersöka vilken effekt det hade på förekomsten av olika former av järn, samt om/hur

arsenat fördelar sig i provet, om det binder till järn eller förblir fritt i lösning. I det fjärde och femte arbetet studerades hur interaktionerna mellan järn och organiskt material påverkar arsenat och fosfat. Till experimenten i dessa två arbeten har kommersiellt tillgängliga naturliga organiska material använts. Röntgenspektroskopi nyttjades för att få information om vilka föreningar som fanns i proverna. Röntgen-spektroskopi bygger på att ljus i ett specifikt energiområde interagerar med elektroner nära kärnan på det grundämne som studeras. Genom att jämföra ljuset före och efter det har interagerat med det specifika grundämnet, t.ex. järn, kan bland annat information om vilka atomer som sitter närmast ämnet av intresse, hur långt borta de sitter och hur många de är erhållas. De olika systemen karakteriserades även med hjälp av totalhaltsanalyser i de naturliga proverna, samt pH-mätningar i samtliga prover.

Två kategorier av järn identifierades i bäckvattnen från försöksparken i det boreala avrinningsområdet (arbete I-III), dels fanns järnmineraler och dels fanns järn som var bundet till organiskt material. Fördelningen mellan dessa två kategorier var olika beroende på den vegetation och jordmån som omgav bäcken. De parametrar som har störst effekt på vilken form av järn som förekommer är koncentrationen av det organiska materialet, pH och totalkoncentrationen järn. De två kategorierna av järn som identifierats i denna studie har tidigare även kunnat påvisas i labbprover, samt i naturliga jord- och vattenprover. Marklösningarna innehöll enbart organiskt bundet järn. I likhet med många av bäckarna så innehöll jordproverna både organiskt bundet järn och järnmineraler. Tillsats av arsenat till bäckvattnet resulterade i en fördelning av arsenat där det dels bildade en utfälld förening med järn ($FeAsO_4(s)$) och dels förblev fri i lösningen och därmed mer biotillgänglig. Denna studie visade att både det organiskt bundna järnet och järnmineralerna påverkades av tillsatsen av arsenat, samt att arsenat förblev i lösning trots att ett överskott av järn fanns i bäckvattnet. Det senare beror troligen på att en del av det organiskt bundna järnet inte var reaktivt mot arsenat, eftersom järnkomplexet med organskt material var så starkt/stabilt.

Liknande resultat erhölls i arbete IV och V, där trekomponentssystemen arsenat eller fosfat, järn och organiskt material studerades. Vid låga järn

koncentrationer var allt järn bundet med organiskt material, vilket resulterade i en stor andel fritt arsenat eller fosfat i lösning. Vid höga järn koncentrationer fanns det både järn bundet med organiskt material och fasta järninnehållande faser. Dessa faser var mest troligt en blandning av järnmineraler och järnutfällningar med antingen arsenat eller fosfat.

Delarbetena som ingår i denna avhandling har bidragit till en bättre förståelse kring vilka former av järn som förekommer i olika miljöer i ett borealt avrinningsområde, vad som styr fördelningen mellan de olika formerna, samt hur fördelningen mellan organiskt bundet järn och järnmineraler påverkar andra ämnen som arsenat och fosfat. Sammanfattningsvis kan sägas att samtliga arbeten har visat på vikten av komplexbildning mellan järn och organiskt material, vilket har geokemisk betydelse för både järn, NOM och ämnen som kan binda till järn eller NOM.

1. Introduction

Iron (Fe) is a highly abundant element on earth and has a significant impact on various biogeochemical processes, e.g. adsorption, desorption, redox, and (co)precipitation with different elements[1]. The speciation significantly affects important parameters such as reactivity, mobility, and availability of metals. Iron may be present as soluble complexes (including hydrated Fe ions), as adsorbed surface complexes, or as solids. The limited solubility of Fe(III) causes a widespread occurrence of Fe minerals in oxic environments. Ferrihydrite, goethite and lepidocrocite are some examples of common Fe minerals[2]. These are characterized by various degrees of crystallinity and density of surface groups. Ferrihydrite is frequently referred to as an amorphous ferric mineral and is the solid Fe phases initially formed in oxic environments. The presence of natural organic matter (NOM) affects the size and structural disorder of naturally occurring ferrihydrite[3]. The properties of synthetic ferrihydrite also depend on prevailing synthesis conditions, e.g. the presence of small organic acids such as citrate or hydroxybenzoic acids decrease the ferrihydrite particle size[4,5]. The presence of NOM has also been shown to induce changes in aggregation properties[6] and mineral crystallinity[6,7]. This has consequences for surface area and reactivity towards nutrients, contaminants and other elements. Furthermore, NOM plays an important role in Fe biogeochemistry via formation of Fe(III)-NOM complexes that suppress Fe precipitation, i.e. formation of reactive surfaces[8,9].

Since NOM strongly influences Fe speciation, it exerts a significant impact on many biogeochemical cycles. Knowledge about Fe speciation in natural systems is important for predicting and/or understanding the fate and bioavailability of Fe, nutrients (e.g. phosphorous), contaminants (e.g. arsenic) and other elements associated with Fe.

1.1 Natural organic matter

NOM may stem from both terrestrial and aquatic environments[10]. It comes from the decomposition of animals and plants[11]. NOM is frequently divided into two groups, namely an insoluble part and a dissolved part, i.e. dissolved organic matter. The exact structure of NOM remains unknown[10] despite numerous characterization attempts, e.g. ref[12]. Amino acids, carbohydrates, carboxylic acids, hydrocarbons and other organic acids have been suggested to account for 20% of the dissolved fraction[12] . Humic acids (HA) and fulvic acids (FA) are suggested to account for the remaining dissolved part. The difference between HA and FA is operationally defined by their solubility properties[10]. FA are typically of lower molecular weight, 300-2000 Da[13], and carry more acidic functional groups. HA have molecular mass values in the range 2000-1 300 000 Da[13]. The negative charges carried by HA and FA leads to a high sorption affinity for Fe- and Al (hydr)oxide surfaces. As previously outlined, binding of NOM to Fe-minerals affects aggregation properties and crystallinity of the mineral[6].

NOM contains a large range of functional groups, such as amide, amine, carbonyl, carboxyl, hydroxyl, phenol and sulfhydryl groups[11,13,14]. Binding properties of these functional groups depend on many parameters, e.g. pKa values and in the case of chelate-structures, distance between functional groups. This implies that NOM may bind a wide range of substances or surfaces and via different groups depending on prevalent conditions. Evidence for dissolved Fe(III)-NOM complexes were presented in 1976 as a plausible explanation for the high concentrations of iron observed in natural waters[15].

1.2 Fe speciation in natural systems

Attempts to describe Fe speciation in natural systems frequently involve simplified model systems consisting of pure minerals or systems with NOM. These model systems represent the two pools of Fe previously described by Karlsson *et al.*, 2012[9]. They suggested the existence of Fe(III)-NOM complexes and polymeric Fe(III) (hydr)oxides. The partitioning between solid and soluble Fe is largely controlled by total Fe concentration, pH and NOM. NOM can suppress hydrolysis of Fe(III), which not only affects bioavailability of Fe, but can also have a great impact on Fe speciation in larger water bodies since the Fe(III)-NOM

complexes are highly mobile in comparison with precipitated Fe(III) (hydr)oxides, which may aggregate and sediment. The chemical nature of the Fe(III)-NOM complexes is commonly described in terms of five- or six-membered chelate ring structures[8,9,16], similar to Fe-oxalate or Fe-malonate structures. Both pools of Fe are reported in studies of natural, oxic, samples such as soils and natural waters.

Iron speciation has been probed using various methodologies. Some examples include electron paramagnetic resonance[17], isotope studies[18,19], flow-field flow fractionation[20,21], and X-ray absorption spectroscopy (XAS)[16,22-26]. These studies focus mostly on Fe(III), which is surprising since both light-induced Fe(III) reduction[27] and microbial activities[28] are likely sources of Fe(II) input. Other sources of Fe(II) may stem from reductive dissolution of ferric minerals. In aerated systems, chemical oxidation via O_2 limits the occurrence of Fe(II). Nonetheless, there are a few studies addressing Fe(II)-NOM complexes, e.g. ref [29].

Fe(II) and Fe(III) constitute a very important redox couple affecting the cycling of many elements[1]. The Fe redox cycling may proceed via biotic[28] or abiotic routes[30]. This cycling involves reduction of Fe(III) minerals to soluble Fe(II) which may remain in solution, form Fe(II) minerals, or be (partly) oxidized via biotic or abiotic routes to form mixed valence Fe(II)/Fe(III) minerals, or new pure Fe(III) minerals[1]. Similarly, oxidation of Fe(II) minerals may result in Fe(III) complexes or precipitates. These reactions are likely to have pronounced effects on the formation of solid Fe(III) phases and thus affect various elements via adsorption, desorption or co-precipitation.

1.3 Arsenic

Arsenic (As) is a potent toxic element that affects the health of millions of people worldwide[31]. Arsenic is found in soils, rocks, minerals, and waters. Elevated As concentrations in the groundwater are found in several countries, e.g. Argentina, Bangladesh, China and Vietnam. In Bangladesh, drilling of shallow wells has resulted in millions of people drinking water that has significantly higher As than the 10 μg l^{-1} guideline of the world

health organization[32,33]. This may lead to adverse health effects such as cancer and skin disorders[31].

The two most environmentally relevant oxidation states in natural waters and soils are As(III), dominating under anoxic conditions, and As(V), dominating under oxic conditions[31]. Due to differences in pKa-values, As(III) is generally considered more mobile as it exists in the fully protonated (H_3AsO_3) species, up to pH 9.2, which limits binding to charged mineral surfaces. In contrast, As(V) carries a negative charge ($H_2AsO_4^-$) from pH ~2 and consequently binds to positively charged mineral surfaces, e.g. Fe, Mn and Al oxide minerals[34,35]. Numerous studies have examined the binding of As(III) and As(V) to mineral surfaces, e.g.[36-46]. The binding is fast and extensive over a wide pH range for both As(III) and As(V). The solubility of As(III, V) bearing phases also limits the concentrations of free As(V) in natural waters. Arsenic is believed to be mobilized through various processes, both from reduction of solid phase As and via mineral dissolution. This contrasts the study of Kocar *et al.,* 2006[47] suggesting that As may be sequestered rather than released upon reductive dissolution of the Fe mineral phase.

Organic material has been shown to strongly influence the transport of As(V), e.g. refs[10,32,48-51]. Sulfhydryl groups in wetland NOM have been shown to form covalent bonds with As(III) under anoxic conditions and thereby immobilize As[52]. Other possible roles of the NOM are i) as substrate for bacteria that reduce Fe and humics, leading to mineral dissolution and desorption of sorbed As-species[10,32,48-51,53], ii) to act as electron shuttles which increase Fe reduction[50], iii) to reduce As(V) to As(III)[54,55], iv) to oxidize As(III) to As(V)[54], v) to bind As(III) and As(V)[56], vi) to compete with As for binding sites[54,57] and vii) to bind As via metal bridges in ternary NOM-Fe(III)-As(III, V) complexes[57-61].

The formation of ternary NOM-Fe(III)-As(V) complexes is frequently ascribed to the increased mobility of As in organic rich environments[10]. The existence of these complexes is often based upon indirect evidence, e.g. strong correlation between Fe, NOM and As[62-64] or results from extractions[65]. These shortcomings were identified by Mikutta *et al.,* 2011[59] who published spectroscopic data suggesting the formation of ternary

complexes constituting As(V) bound to small polymeric clusters of Fe that were bound by NOM. Furthermore, a recent publication suggests the existence of corresponding As(III) complexes[61]. To summarize, most studies suggests that NOM increases As mobility, but the exact routes are under debate.

1.4 Phosphorous

Phosphorous (P) is an essential element conducting important functions in organisms, such as being a significant constituent of cell membranes, as an energy mediator in the form of ATP/ADP/AMP in cells and as encoders of genetic information in the form of DNA. Phosphorous is also very important from an agricultural point of view. Phosphorous is frequently a limiting nutrient in the production of crops as only a limited fraction of P present in the soil is bioavailable. Alternately, eutrophication is an adverse effect caused by elevated P concentrations. Inorganic P typically occurs in the form of P(V), i.e. $H_2PO_4^-$ or HPO_4^{2-} at most environmentally relevant pH values. Phosphorous concentrations in the environment are limited by P adsorption onto surfaces and P co-precipitation with e.g. Fe(II), Fe(III) or calcite. These processes are well known, e.g. ref [66], and involve cycling between Fe(II) and Fe(III), surface binding, as well as co-precipitation reactions resulting in vivianite, iron phosphate and/or calcite precipitates. Phosphorous (V) displays similar characteristics as its As(V) analogue, e.g. both bind strongly to Fe and Al-minerals[67,68]. This has implications for As removal via Fe-minerals, in places like Bangladesh, where high levels of P and other ions with high binding affinity (e.g. silicate) may occur in groundwaters[69,70]. In accordance with As studies, organic material might compete for surface binding sites on Fe(III) (hydr)oxides and thus affect P binding[71-74]. Furthermore, organic material may complex Fe and prevents formation of reactive mineral surfaces, which would have an even more pronounced effect on P cycling.

1.5 XAS

X-ray absorption spectroscopy (XAS) is based on absorption of X-rays. During data acquisition, the sample is scanned over a specific energy range, e.g. ca: 6 880-7 800 eV for Fe K-edge and 11 630-12 700 eV for As K-edge. Typical XAS spectra are outlined in Figure 1. Initially, almost no X-rays are absorbed. When the energy of an X-ray equals the binding

energy of a core electron, then there is a sharp increase in absorption; this is called the absorption edge. The binding energy of the core level electrons varies for the elements, and it is possible to study electrons in different shells, e.g. 1s (K-edge) and 2s/2p (L-edge). Some elements display pre-edge features, (e.g. Fe) that are due to electronic transitions within the atom to energy levels that are unfilled or partly filled. The pre-edge and the edge (+ some additional 50 eV after the edge) comprise the X-ray absorption near edge structure (XANES) region which can reveal key features including oxidation state and coordination environment. The oscillating structures near and after the edge are caused by backscattered photoelectrons. The region after the edge is called the extended X-ray absorption fine-structure (EXAFS) region. The photoelectrons are ejected when the energy of the incoming X-rays are higher than the binding energy of the core electron. Excess energy is then released kinetically in the form of an ejected photoelectron. The photoelectron may then scatter on neighboring atoms and depending on the distance, number and identity to/of the backscattering atoms, the interference between ejected and backscattered photoelectrons may differ. Therefore, EXAFS analysis provides information about the identity of the neighboring atoms, coordination number (CN), as well as the distances at which they occur. XAS is element specific and could be applied to solids, liquids, and gaseous samples. In contrast to techniques such as X-ray diffraction, XAS can be applied to both amorphous and crystalline samples, making it a very versatile technique. More information about XAS could be obtained from e.g. ref[75].

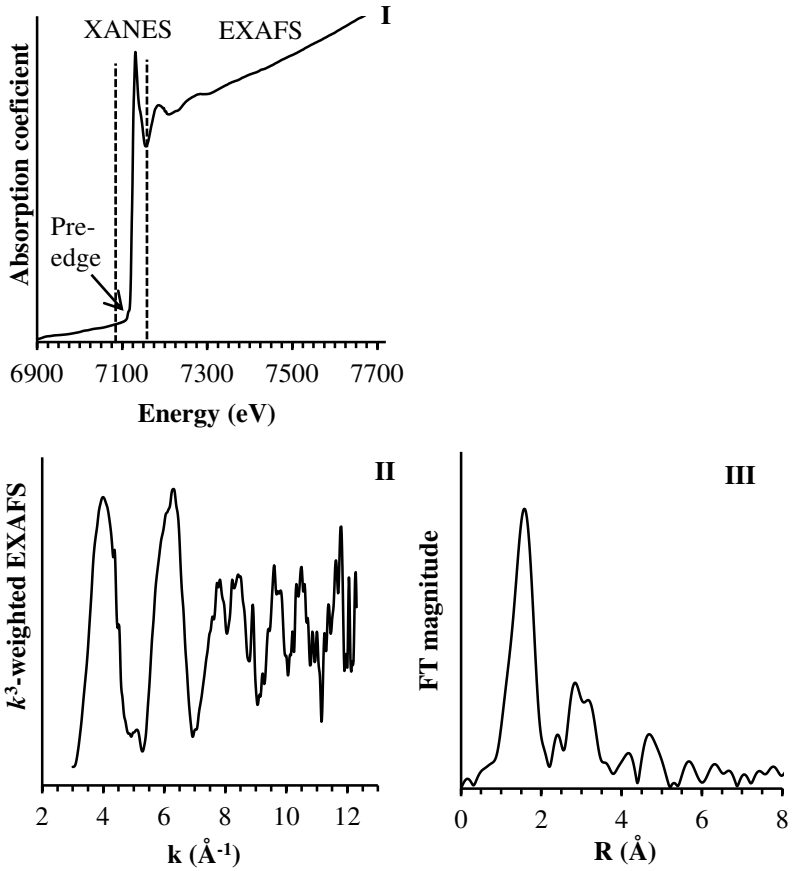

Figure 1. XAS data of S4 soil (0-10 cm from surface) from the Krycklan Catchment according to I) Raw data, II) k^3-weighted EXAFS, and III) the corresponding Fourier transform.

1.6 Krycklan Catchment

The Fe-speciation studies on natural samples in Papers I-III were based on samples collected in the Krycklan catchment. It is a well-studied boreal catchment situated at 64°, 16'N, 19°46'E[76,77]. The Krycklan Catchment provides infrastructure for long-term studies within the catchment[77]. There are several sub catchments within the Krycklan Catchment, for maps and more information see ref[78]. The sub catchments have been characterized with respect to stream order, area, and percentages of lake, forest and wetland, as well as landcover type[77,78]. According to Buffam *et al.,* 2007[78]: "Landcover type was defined by percent wetland coverage,

with <2% wetland “forested”, 2-30% wetland “mixed”, and >30% wetland “wetland.””. The water chemistry depends on the catchment characteristics, as well as stream size. A recent publication by Neubauer *et al., 2013*[20] showed how pH and iron speciation vary within the catchment depending on stream order. Parameters important for stream water chemistry, e.g. pH, dissolved organic carbon (DOC) and major anions and cations have been analyzed on a regular basis since 2002[77]. The importance of DOC characteristics, as determined by its origin, i.e. surrounding landscape element, have been demonstrated in several publications, e.g. refs[79,80]. Seasonal variation of Fe has also been studied at a forested (C2) and a wetland site (C4) and a strong correlation between Fe and DOC was found in the C2 site[81]. The corresponding correlation in the wetland stream was lower (r^2 =0.32 for Fe_{tot}, compared with r^2=0.77 for the corresponding forested stream).

The forest soils are dominated by iron podzols, but the streams are surrounded by a riparian peat zone that contains more organic material[77]. Drainage of the riparian zone during spring flood have been proposed as the mechanism causing elevated DOC levels in forested streams[82]. In contrast, DOC levels in wetlands decline during spring flood[81].

2. Outline of this thesis

This thesis focuses on Fe interactions with organic material and how it affects Fe speciation and reactivity. There are few studies where Fe speciation has been studied in natural waters. This is due to the low native concentrations that prevent the collection of molecular scale information, e.g. to obtain Fe K-edge XAS data. Therefore, a gentle and non-invasive protocol for concentrating Fe-species in natural waters was developed and evaluated (Paper I). This technique was later applied to natural water samples from the well-studied Krycklan catchment. The applicability of the technique was demonstrated using a gradient of stream water samples from one stream (Paper I). Previous studies within the Krycklan catchment have shown differences in the properties of e.g. DOC[80] and bacterial growth[79] in the streams depending on the landscape characteristics forest and wetland that surround the streams. Therefore, to investigate whether similar differences could be observed for Fe-speciation 5 streams water samples, originating from forested, wetland and a mixed site streams, were studied (Paper II). In the same paper, Fe speciation was followed at one location from the soil, to the soil solutions, groundwater and out to the stream. Fe reactivity in the stream was further analyzed by adding As(V) to stream water at various Fe to As ratios (Paper III). The fate of As(V) and P(V) are strongly linked to the speciation of Fe. Since the speciation of Fe is dependent on parameters such as pH and total Fe concentration, the interactions between Fe, As(V) or P(V) and NOM were studied over a large experimental range including variation in Fe concentration, Fe/As or Fe/P ratios and pH (Papers IV and V).

3. Materials and Methods

3.1 Chemicals, solutions and pH measurements

The chemicals used for these studies were of p.a. quality unless stated otherwise. All experiments were conducted in a 25°C thermostated lab. The solutions were prepared with boiled Milli-Q-water. For the work with model metal complexes (Paper 1), which were based on thermodynamic calculations, the ionic strength was kept constant with 100 mM NaCl. pH measurements of these solutions were conducted using a 100 mM NaCl combination electrode in order to reduce errors caused by junction potentials. The electrode was calibrated with an E_0-solution, i.e. a solution with a coulometrically determined H^+-concentration. Other pH measurements were conducted with 3 M KCl combination electrodes (i.e. a 3M KCl Orion Ross, a Mettler Toledo DGI 112-Pro combination electrode, and a Mettler Toledo InLab®Micro pH combination electrode). The electrodes were 2-point calibrated at pH 3 and 7 with commercial buffers. The NOM used in Papers IV and V was purchased from the International humic substances society. Three kinds of NOM were studied, Pahokee Peat humic acid (PPHA, 1R103H), Suwannee River NOM (SRN, 1R101N) and Suwannee River Fulvic acid (SRFA, 1S101F). The Pahokee Peat is an agricultural peat soil and the humic acid is isolated via an alkaline extraction, where the humic acids were precipitated at pH 1 and then desalted and freeze-dried. The Suwannee River materials stem from a blackwater river, with high DOC (25-45 mg/l) and low pH (<4). Due to differences in the isolation procedure, the composition of SRN and SRFA differs. The SRN material was isolated via filtration followed by reverse osmosis and freeze-drying and contains hydrophobic and hydrophilic acids and soluble organic solutes[83,84]. A multistep isolation procedure was conducted for isolation of the SRFA material[85]. In summary, acidified river water was repeatedly passed over a XAD-8 resin, eluted with NaOH and re-acidified with HCl. To remove Na^+, the fulvic acid eluate was passed over a hydrogen-saturated cation-exchange resin before freeze-drying. Since the XAD-8 resin adsorbs hydrophobic compounds, the SRFA material only contains hydrophobic organic acids[86]. The work with natural stream water samples was conducted using acid washed plastic or glass laboratory containers.

3.2 Thermodynamic calculations

Thermodynamic calculations were performed in WinSGW[87], which is based on SolGasWater[88]. The calculations were conducted in Paper I, IV and V. The program performs equilibrium calculations according to the free-energy minimization method. It describes the chemical equilibria as equation [1], which is a combination of the law of mass action and the equilibrium reaction. For the modeling, the stability constants were recalculated to be valid at the correct ionic strength.

$$[A_pB_qC_r] = \beta_{pqr} * a^p b^q c^r \qquad [1]$$

where $[A_pB_qC_r]$ is the concentration of the formed equilibrium species, β_{pqr} denotes the equilibrium or formation constant for the formed complex and a, b and c corresponds to the concentration of components.

In Papers IV and V models describing the speciation in the binary Fe(III)-NOM and ternary As(V)/P(V)-Fe(III)-NOM systems were obtained. According to IR spectroscopy studies, all carboxylic acid groups in the SRFA and SRN materials are not reactive towards trivalent metal ions[89]. In Papers IV and V, the reactive fractions of carboxylic acid groups from the SRFA and SRN material were assumed to be 15 and 20 %, respectively. The composition and stability of the Fe(III)-NOM complexes, and solid solutions according to Thibault *et al.,* 2009[90] were optimized. The stability of $FeAsO_4$(s) and $FePO_4$(s) were also optimized. Literature values were used for the rest of the components. The input data for the modeling consisted of measured pH values, total concentrations of As(V), Fe(III), P(V), reactive dicarboxylic groups, soluble concentrations of $H_2AsO_4^-$ or $H_2PO_4^-$ from IR spectroscopy and the presence of Fe(III)-NOM complexes or solid phases according to EXAFS data analysis. The stability constants were optimized by minimizing the total residual sum of square.

3.3 Preconcentration protocol

The low native concentrations of Fe in natural stream waters prevent direct XAS investigations. This calls for a need of preconcentration procedures. A frequently used method for preconcentration is filtration, which can also be combined with freeze drying. This is procedure can

however induce artifacts such as changes in the partitioning pattern, e.g. more crystalline fractions[91-93]. It may also cause oxidation of the sample[92]. Therefore, a more gentle protocol based on the driving force of electrostatics was developed. Electrostatic adsorption of complexes, e.g. $Pb(EDTA)^{2-}$, onto surfaces has previously been shown not to induce differences in the closest coordination sphere[94,95].

Three commercially available resins from Dowex were purchased. Two of the resins were based on the same functional group, a trimethylamine (TMA) group. These were Dowex 1x2, chloride form, p.a., 200-400 mesh (Fluka), denoted TMA1 and the Dowex 1x8 chloride form, 200-400 mesh (Sigma Aldrich), denoted TMA2. The level of cross-linking, 2 and 8 % respectively, differed between these two resins. Dowex Marathon A2 chloride form, 30-40 mesh, was based on dimethylethanolamine (DMEA) as functional groups and therefore denoted DMEA. Hence, TMA1 and 2 differ from DMEA in terms of functional group and size. 30-40 mesh corresponds to particle sizes of 595-400 µm and 200-400 mesh corresponds to particle sizes of 74-37 µm. Particle size is of importance not only for the adsorption but also for the acquisition of XAS data in transmission mode, as artefacts may occur if the particle size is too close to an absorption length of the light interacting with the sample[75]

The preconcentration involved a few basic steps. In the initial step, a fixed mass of resin was weighted into a clean test tube. The resin was then wetted/washed 3 times with MilliQ-water or 0.1 M NaCl solution, depending on which type of sample that would be pre-concentrated in the subsequent step, and centrifuged 1 minute at 5000 rpm between each wetting/washing. The resins were then added to the sample solution. Redox sensitive samples were handled in a glove box or under an atmosphere of N_2 gas. Samples at risk of being reduced by light, i.e. all Fe containing samples, were covered with aluminum foil. All samples with volumes ≤ 50 mL were then placed on an end-over-end rotator for 24 hours. Larger sample volumes, i.e. the natural stream waters, soil solutions and ground water, were manually rotated several times per day for 5-7 days. For small samples (≤ 50 mL), the adsorption process was terminated by centrifuging the samples for 5 minutes at 5000 rpm and then decanting the majority of the solution and transferring the resins with adsorbed complexes into a smaller test-tube. For the larger sample volumes, the resins were first allowed to sediment overnight (this time was included in the adsorption time) and then the majority of the solution

was decanted. The remaining solution and resins were transferred to a 50 mL falcon test tube and then centrifuged 5 minutes at 5000 rpm and processed as described for the small sample volumes. Throughout the process redox sensitive samples were handled under a N_2 atmosphere and covered with aluminum foil whenever possible. Aliquots for total concentration measurements of total organic carbon (TOC) and metals were taken after adsorption in order to establish the amount adsorbed. For natural samples, aliquots for pH, TOC and metal concentration determinations were taken prior to the adsorption as well. TOC was measured on a Shimadzu TOC-V CPH analyzer and a Shimadzu TOC 5000. Metal concentrations were determined on a Perkin Elmer Atomic Absorption Spectrometer 3110 and a Perkin Elmer SCIEX ELAN DRC-e ICP-MS.

3.3.1 Characterization of preconcentration protocol

The preconcentration protocol was characterized with respect to effect of functional group and level of crosslinking on the resins, surface loading of complexes and the chemical nature of the complexes. All three resins, TMA1, TMA2 and DMEA, were tested. Since the method is based on electrostatic adsorption all complexes have to carry negative charge(s) to be able to sorb onto the resins. The evaluation set of representative metal complexes consisted of $Fe(C_2O_4)_3^{3-}$, $Cu(C_2O_4)_2^{2-}$, $Cu(C_{10}H_{12}O_8N_2)^{2-}$ and $Mn(P_2O_7)_2^{5-}$. Thermodynamic calculations in WinSGW established the ratio of metal and ligand concentrations, as well as pH, needed for the metal-ligand complexes to completely dominate the aqueous speciation. The XAS spectra of metal-ligand complex solutions were then compared with the spectra of the adsorbed complexes.

WinSGW calculations were also conducted to elucidate appropriate metal ligand ratios in a mixed metal ligand solution comprising equal amounts of $Fe(C_2O_4)_3^{3-}$ and $Cu(C_2O_4)_2^{2-}$ with respect to the metal ions. For both Fe^{3+} and Cu^{2+}, their respective $C_2O_4^{2-}$ complexes constituted ≥99% of the metal ion speciation. The mixed metal ligand solution was used for a competitive adsorption study, where the mass of the resin was kept constant, whereas the volume of the mixed metal ligand solution was gradually increased. Increasing the sample volumes results in more complexes binding to the resin and at a certain point the resin becomes saturated with respect to available binding sites. At this point, the Fe- and Cu-complexes start to compete for binding sites. The competitive effect was evaluated by measuring metal concentrations left in solution after adsorption. Similar competitive binding situations are likely in natural waters containing large

quantities of NOM with charged functional groups that could potentially bind to the resins.

3.4 Collection and preparation of samples from the Krycklan Catchment

The stream water samples from the Krycklan Catchment were sampled at various times during low flow conditions in autumn and early winter between 2009 and 2012 (Papers I-III). All stream water samples were collected in acid washed polyethylene flasks that were rinsed three times with stream water prior to filling under the water surface. The flasks were filled to the brim to reduce the effect of headspace air. They were then kept cold and in the dark during transportation and storage. The natural stream water samples were pre-concentrated on TMA2, as it was most efficient in binding Fe species from natural samples (Paper I).

In order to elucidate possible effects of competitive adsorption and/if different Fe species were present in different fractions of the stream water a gradient series was constructed based on 20 L of stream water, sampled at C2 in February 2010 (Paper I). The procedure was similar to that of the competitive binding experiment with $Fe(C_2O_4)_3^{3-}$ and $Cu(C_2O_4)_2^{2-}$. Briefly, the mass of resins was kept constant at 0.500 g and the volumes of stream water added to the resins were approximately 50, 100, 200, 400, 800, 1200, 1600, 2000, 4000 and 8000 mL. The gradient samples were then characterized with regard to the adsorption of Fe and DOC and representative samples were chosen for XAS measurements.

In Paper II, concurrent sampling of soil, soil solutions, groundwater, and stream water from the C2 site was performed in an attempt to characterize Fe speciation in adjacent landscape elements. The soil samples were collected in double plastic bags, cooled and stored in a freezer until shipping for XAS measurements. The soil solutions and groundwater were collected using suction lysimeters as described in Ågren *et al.,* 2008 (ref[96]). To reveal possible linkages between Fe speciation in stream water and land cover type, C1, C2, C3, C4 and C10 were sampled in January 2012 (Paper II).

To study how Fe and As speciation varies as a function of Fe/As ratio, natural stream waters from C2, sampled December 2010, were spiked with a pH-adjusted As(V) stock solution (Paper III). Fe/As ratios were

1.9, 3.6 and 13.0. The spiked stream waters were equilibrated for 24h prior to addition of resins. One native sample was used as a reference.

3.5 Preparation of As(V)/P(V)-Fe(III)-NOM samples

The aim of these studies was to investigate the speciation in the ternary As(V)/P(V)-Fe(III)-NOM systems. More specifically, the situation where the oxyanion was added after the formation of Fe(III)-NOM-complexes and precipitated iron mineral phases was studied. Three different sources of NOM were used, PPHA, SRN and SRFA. To better understand the speciation in these complex systems they were compared to reference systems containing only Fe(III) and NOM. The Fe(III)-PPHA system and the Fe(III)-SRN system are already published[8,9]. The corresponding Fe(III)-SRFA system included in Paper IV was prepared using the same protocol. Briefly, 30 mg SRFA was weighted into a 1.5 mL eppendorf test tube. Then Milli-Q-water and an acidified iron stock solution were added to yield the target Fe loading. The sample was mixed and equilibrated at low pH for approximately 20 minutes in order to allow Fe(III)-NOM complexes to form. Then pH was raised by NaOH addition and subsequent mixing. The sample containers were covered with aluminum foil and equilibrated on an end-over–end rotator for 2 hours, prior to upright equilibration for another 20 hours. The pH was then measured with a calibrated combination micro-electrode. If necessary the pH was readjusted and the sample was re-equilibrated as previously described. Final pH was determined as the pH obtained on the third day after the last pH-adjustment and final dilution with Milli-Q-water to reach target volume and concentrations.

The protocol for the oxyanion samples was very similar. However, when the Fe had equilibrated with NOM (24 hour), oxyanion stock solution was added. If necessary, pH was readjusted after equilibration. The samples were stored in a fridge for 1-3 weeks prior to EXAFS measurements. IR spectroscopy samples were stored for 1-3 days prior to measurements. For selected samples, pH was re-measured 3 weeks after preparation to ensure the pH did not drift and the value was identical with that obtained 3 days after pH adjustment. This suggests that the samples are equilibrated relatively quickly and that sample storage for shorter periods of time should not affect sample speciation.

3.6 Collection and analysis of XAS data

All XAS data was collected at beamlines 4-1 and 4-3 at Stanford Syncrotron Radiation Lightsource (SSRL), California, USA. SSRL was operated in top-up mode at 3.0 GeV beam energy and 150-350 mA ring current. Three ion chambers filled with N_2 were used to monitor the transmitted beam and a Lytle detector (filled with Ar) was used for fluorescence measurements. The beam was monocromatized by a double crystal monochromator, Si [2 2 0], $\Phi = 90$ at 4-1 and Si [1 1 1], $\Phi = 90$ at 4-3. At 4-1, higher order harmonics were reduced by detuning the monochromator (30-50%) and at 4-3, a nickel coated harmonic rejection mirror was used for the same purpose. All XAS spectra were collected in fluorescence and transmission mode. Therefore, the samples were aligned at 45° with respect to the incoming beam. Unwanted scattering and fluorescence contributions were reduced by filters according to the Z-1 principle, where Z is the atomic number for the element to be measured, e.g. a Mn filter was used for Fe, a Cr filter was used for Mn, a Ge filter was used for As and a Ni filter was used for Cu. To allow for internal calibrations, the spectra of a reference foil, e.g. Fe, was collected simultaneously as the spectra for the sample. All spectra were energy calibrated and evaluated with respect to beam damage. Most spectra represent the average of ~3-30 individual, energy-calibrated, spectra. The higher numbers account for recording Fe-XAS data from natural stream water, soil solution or ground water samples from the Krycklan Catchment. Furthermore, fluorescence and transmission spectra were compared to verify that the spectra were not affected by self-absorption. XAS data analysis, performed on fluorescence spectra, included linear combination fitting (LCF), XANES, pre-edge and wavelet transform (WT) analysis and shell-by-shell EXAFS data fitting.

3.6.1 XANES and pre-edge analysis

As previously outlined, the XANES region can reveal information about oxidation state and symmetry of the local environment for an element. XANES analysis can be conducted differently, e.g. visual comparison of the normalized absorbance, study of first derivative normalized absorbance, LCF of the XANES region or by detailed analysis of the pre-edge region as outlined by Wilke *et al.,* 2001[97]. LCF will be described in more detail under the EXAFS section. In this thesis, a combination of the other three methods for XANES analysis has been applied. In Papers I and III-V the XANES region was studied in the normalized absorbance and

first derivative absorbance spectra to identify similarities and differences between samples and/or samples and model compounds. Samples with identical coordination environment and oxidation state will display identical XANES spectra. The position of the pre-edge and edge are indicative of oxidation sate, hence a comparison between reference compounds of known oxidation state, and samples might help identify the prevailing oxidation state in the samples. A more detailed procedure to identify Fe oxidation state, i.e. differentiate between Fe(II) and Fe(III) have been presented by Wilke *et al., 2001*[97]. This method was applied in Paper II. Briefly, the centroid position was extracted from normalized and baseline subtracted spectra by adjusting a baseline around the pre-edge and then fit the pre-edge with pseudo-Voigt functions. Peak area and position were used to calculate the centroid.

3.6.2 Wavelet transform

Wavelet transform analysis performed in Papers I-V is based on an Igor Pro script developed by Funke *et al.,* 2005 (ref[98]). The WT is a complement to FT, which resolves backscattering atoms based on their distance from the absorbing atom. In contrast, the WT also resolves in *k*-space, which enables separation of light and heavy atoms present at the same distance[98]. For example, Fe-WT enables qualitative differentiation between C and Fe backscattering atoms[8,9,16]. The result of the WT analysis is typically represented by a contour plot, where ridges represent regions where a particular pair of absorber and backscatterer have contributions in both R- and *k*-space[16]. The position of the ridges enables discrimination of different backscatters. Therefore, WT for model compounds are typically part of the WT analysis. An overview of the WT results for ferrihydrite is presented in Figure 2, where both a WT and a high-resolution WT only containing contributions from second and third shells, are included.

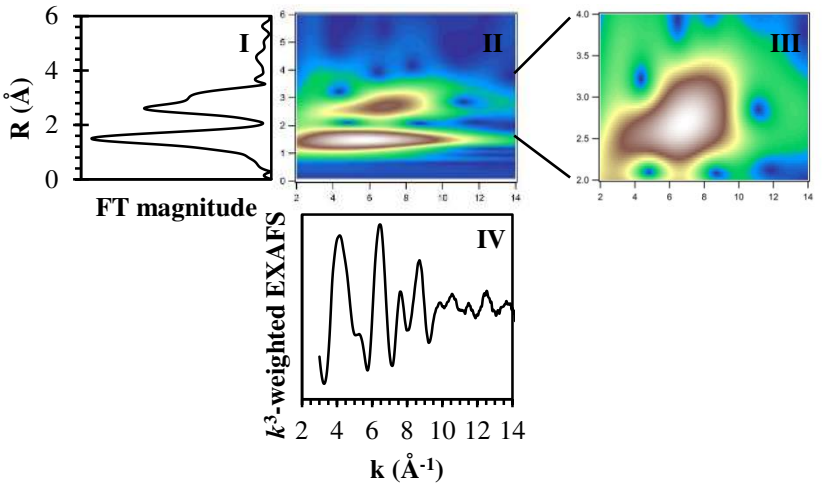

Figure 2. Overview of the WT modulus of ferrihydrite with I) FT spectrum, II) WT (η=8, σ=1), III) high resolution WT (η=8, σ=1) and IV) k^3-weighted EXAFS spectrum. The WT are plotted as a function of k (Å^{-1}) on the x-axis and as a function of R (Å) on the y-axis.

3.6.3 EXAFS

EXAFS data analysis was conducted in Viper[99] for shell-by-shell data fitting and in SixPack[100] for LCF. Data reduction was performed on k^3-weighted spectra, which enhances the oscillations at higher k-values. The principle for LCF is that an experimental spectrum is fitted by a linear combination of reference spectra. This could be conducted on spectra from both the XANES and EXAFS regions and is strongly dependent on reference spectra, i.e. it is important to have representative reference spectra. In Papers II and V, LCF was conducted on k-space data in the EXAFS region using non-negative boundary conditions and floating E_o. Components contributing less than 1% in the LCF were excluded. Furthermore, since the model compounds were not likely to fully explain the experimental spectra, the sum was not forced to equal 1. In Paper II, LCF was conducted on k^3-weighted spectra from k 3.0 to 11.0 Å^{-1} using biotite, ferrihydrite, goethite, hematite and a 6489 ppm Fe SRN sample at pH 5 as reference spectra. In Paper V, the spectra were fitted in the k-range 2.8-12.0 Å^{-1}, using a 6489 ppm Fe SRN sample at pH 5, ferrihydrite, goethite, hematite and amorphous ferric phosphate as reference compounds.

For shell-by-shell data fitting in Viper[99], the initial stages included pre- and post-edge subtraction of first-order polynomials and normalization. For background subtraction, a smoothing spline function was added above the absorption edge. The spectra were Fourier transformed using a Bessel window. In Papers I and II a region in the 0.6-3.7 range was back-filtered into *k*-space. In contrast, in Papers III-V spectra were not back-filtered. An advantage of back-filtering is that it may remove contributions from long-distance scatterers. Back-filtering is advantageous to apply on series of samples having different quality of the spectra. However, it may also induce artifacts, so the procedure should be applied with care and it may be beneficial to apply fitted results to both filtered and non-filtered experimental spectra. Non-linear least-square refinements with parameters obtained via ab-initio FEFF7[101] calculations were used to analyze filtered and non-filtered spectra. The input structures for the FEFF7 calculations were biotite[102], goethite[103], scorodite[104], strengite[105], and trisoxalatoiron(III)[106]. The amplitude reduction factor S_0^2 was determined by filtering and fitting the first shell in a sample where the first shell CN is known and then adjusting S_0^2 until that value was reached. In order to restrict the number of free variables, values were correlated or fixed when available. For example, the wide occurrence of carboxylic groups in NOM motivates a correlation between the single scattering Fe-C path and the multiple scattering Fe-C-O path, in accordance with carboxylic like structures. Furthermore, the Debye-Waller factors (σ^2) were fixed to literature values, i.e. 0.0056 for Fe-C (ref[106]), 0.0100 for Fe-Fe (ref[107]) or to values determined separately for reference compounds. Therefore, the number of free variables never exceeded the limit given by the Nyquist theorem ($N_{max}=2\times\Delta k\times\Delta R/\pi$, where Δk represents the *k*-range in the EXAFS spectrum and ΔR is the R-range of the FT range).

3.7 Infrared spectroscopy

A Bruker Vertex 80 vacuum spectrometer equipped with a DTGS detector was used for infrared (IR) measurements in attenuated total reflection mode. The measurements were conducted in a 25.0 ±0.15°C thermostated room. A ZnSe crystal was used as an internal reflection element. The As(V)/P(V)-Fe(III)-NOM samples (in Papers IV and V) were transferred to the crystal surface using a pipette and then protected from the atmosphere using a stainless steel lid. For each sample 1000 scans were recorded in the range 400-5000 cm^{-1} at a resolution of 4 cm^{-1}. In

addition to the samples from the ternary sample series, the spectra of pH-adjusted 0.27 M NaCl solutions, SRN dissolved in water adjusted to pH 3 and 6, and SRFA dissolved in water adjusted to pH 3 and 6, were also recorded. These spectra were used for subtraction of the water and organic material contributions in the sample spectra.

IR spectroscopy was used to quantify the concentrations of free As(V) and P(V) in the samples. Spectra of aqueous $H_2AsO_4^-$ and $H_2PO_4^-$ at 1-250, 2-128 mM, respectively, were recorded for construction of calibration curves. The area of the As bands and the height of the P bands were correlated to the area of the OH bending vibration in water around 1600 cm^{-1}. The peaks of the P bands overlapped with peaks from the SRN material and from the $FePO_4(s)$. Therefore, the spectral contributions of these two compounds were subtracted from the sample spectra prior to baseline correction and peak height analysis.

4. Results and Discussion

The results from the studies comprising this thesis all highlight the importance of Fe complexation via NOM, which suppress Fe precipitation. This is in line with several recent studies on Fe speciation[8,9,16,20,21,23,25,108]. Three of the papers (Papers I-III) were based on a preconcentration protocol which was shown to not induce any major distortions in the inner coordination sphere, thus providing a protocol for preconcentration of Fe in natural waters prior to XAS analysis (Paper I). Furthermore, a recent publication reveals that Fe-speciation results obtained via concentration on resins are in better agreement with results obtained via thermodynamic calculations compared to speciation results obtained from freeze-dried samples[23]. The preconcentration protocol will first be briefly discussed, then the results from the studies within the Krycklan catchment are presented (Papers I-III), and finally, the results for the ternary oxyanion(V)-Fe(III)-NOM systems (Papers IV-V) will be discussed.

4.1 Evaluation of preconcentration protocol

The electrostatic adsorption of the metal-ligand model complexes to the positively charged resins did not induce any structural or compositional changes (Paper I). No structural or compositional effect was observed for binding to different functional groups (i.e. TMA or DMEA), for different

amounts of adsorption or for binding to resins with different levels of crosslinking (i.e. TMA1 or TMA2), representative spectra of $Fe(C_2O_4)_3^{3-}$ in Figure 3. The $Mn(P_2O_7)_2^{5-}$, $Cu(C_2O_4)_2^{2-}$, and $Cu(C_{10}H_{12}O_8N_2)^{2-}$ complexes represent other structural and electronic properties than $Fe(C_2O_4)_3^{3-}$. Therefore, the lack of discrepancies when comparing solution spectra with the spectra obtained for the adsorbed complexes indicates that the ion exchange resin protocol is applicable over a wide range of complexes with different chemical, structural, and electric properties. The competitive binding experiment with $Fe(C_2O_4)_3^{3-}$ and $Cu(C_2O_4)_2^{2-}$ revealed a charge-dependency in the adsorption to the resin. Briefly, at low surface loadings both Fe- and Cu-complexes adsorbed to the resins, but at increased surface loadings the more negatively charged Fe-complexes gradually out-competed the Cu-complexes (Figure 4). This has implications for binding of Fe-complexes from natural waters, i.e. there might be selectivity effects and there is a significant risk that Fe-complexes will be out- competed by DOC or other, negatively charged, metal complexes.

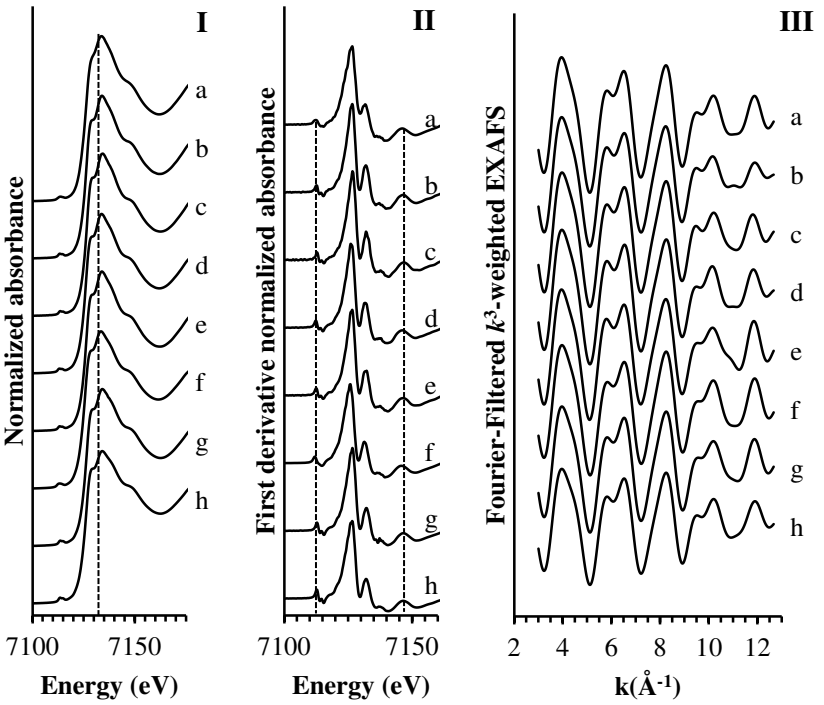

Figure 3. I) Normalized absorbance, II) first derivative normalized absorbance, and III) k^3-weighted Fourier filtered EXAFS data of the $Fe(C_2O_4)_3^{3-}$ system according to a) $Fe(C_2O_4)_3^{3-}$solution, b) 2.2 mg g^{-1} $Fe(C_2O_4)_3^{3-}$ on DMEA, c) 2.8 mg g^{-1} $Fe(C_2O_4)_3^{3-}$ on TMA1, d) 2.8 mg g^{-1} $Fe(C_2O_4)_3^{3-}$ on TMA1, e) 5.6 mg g^{-1} $Fe(C_2O_4)_3^{3-}$ on DMEA, f) 13.9 mg g^{-1} $Fe(C_2O_4)_3^{3-}$ onTMA2, g) 14.0 mg g^{-1} $Fe(C_2O_4)_3^{3-}$ on DMEA, and h) 22.1 mg g^{-1} $Fe(C_2O_4)_3^{3-}$ on DMEA. This figure is modified from Paper I.

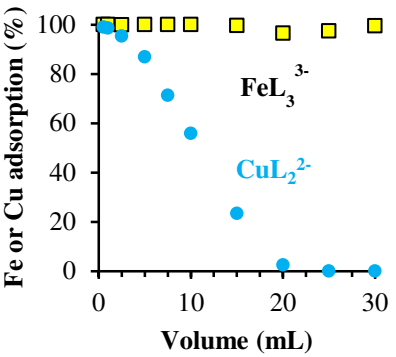

Figure 4. Competitive adsorption between $Fe(C_2O_4)_3^{3-}$ (yellow squares) and $Cu(C_2O_4)_2^{2-}$ (turquoise circles) to functional groups (i.e. binding sites) at the resins as a function of volume added of a 2.5 mM Cu^{2+}, 2.5 mM Fe^{3+} and 20.0 mM $C_2O_4^{2-}$ solution. L=$C_2O_4^{2-}$. This figure is modified from Paper I.

4.2 Fe speciation in the Krycklan Catchment

Fe speciation within the Krycklan catchment showed great variability (Papers I-III). In addition to the two pools of Fe (Fe(III)-NOM and Fe(III) (hydr)oxides) previously identified by Karlsson *et al., 2010*[8], data presented in Paper I suggest the existence of two or more subspecies within each pool, i.e. Fe(II, III)-NOM complexes and precipitated Fe. This was confirmed in the experiment where increasing volumes of C2 stream water was added to a fixed mass of resin, Table 1. Previous studies within the catchment have emphasized the influence of surrounding landscape on the properties of DOC in stream water[79,96]. In accordance with those studies, the speciation of Fe in stream water differed between forested and wetland sites. Stream water from the forested sites comprised both Fe(II, III)-NOM complexes and precipitated Fe(III) (hydr)oxides, whereas the stream waters originating from wetland sites only contained organically complexed Fe. The approach to characterize Fe speciation in adjacent landscape elements revealed that Fe(II) was a significant constituent of the total Fe content. That study also highlighted the importance of NOM complexation for suppressing Fe precipitation. Spiking the stream waters with As(V) resulted in changes in Fe speciation. Increasing concentrations of As(V) resulted in a gradual increase of a $FeAsO_4$ phase. An overview of the Fe-speciation samples from the Krycklan Catchment that are part of this thesis is presented in Table 1. In contrast to previous work on Fe speciation in natural environmental samples, our detailed pre-edge

analysis[97] revealed that some of the samples in this study contained a significant fraction of Fe(II) (Figure 5).

Table 1. Overview of liquid samples collected from the Krycklan catchment.

Sample	pH	Fe (µM)	DOC (mg/L)	Landcover[a]
S4 soil sol., 20-30 cm[b]	4.3	39.4	42.3	Forest
S4 soil sol., 50-60 cm[b]	4.4	54.4	25.3	Forest
Ground water[b]	4.4	17.6	22.3	Forest
C2 stream water[b]	4.5	16.5	18.7	Forest
C2 stream water[c]	5.9	8.4	11.2	Forest
C2 stream water[d]	5.5	29.7	13.9	Forest
C1 stream water[e]	4.9	19.1	15.5	Forest
C2 stream water[e]	5.4	9.8	12.0	Forest
C3 stream water[e]	4.3	9.8	39.9	Wetland
C4 stream water[e]	4.6	16.2	28.9	Wetland
C10 stream water[e]	5.8	19.1	13.4	Mixed

Distances refer to distance from ground level.

[a] According to Buffam *et al., 2007*[78].

[b] Sampled October 2009 for Fe speciation study within adjacent landscape elements.

[c] Sampled January 2010 for study of Fe speciation in C2 stream water.

[d] Sampled December 2010 for study of Fe- and As speciation at C2.

[e] Sampled January 2012 for study of effect of surrounding landscape elements.

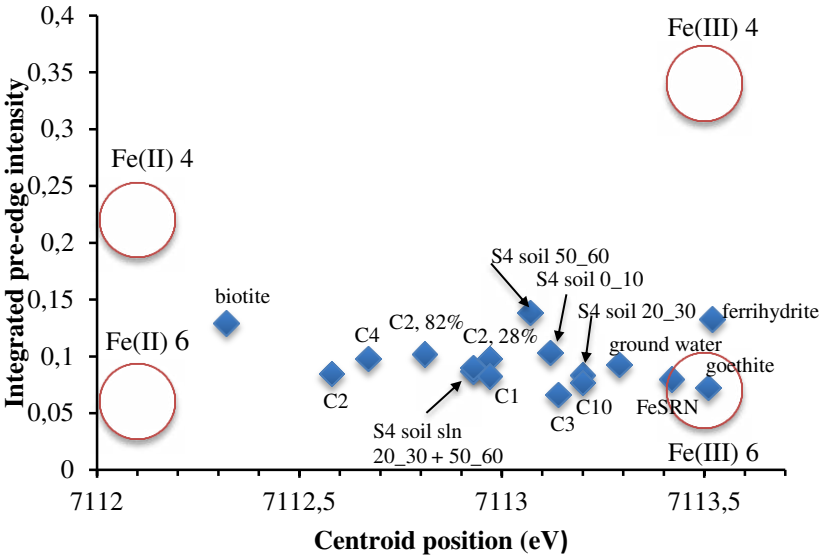

Figure 5. Pre-edge analysis of the samples, from adjacent landscape elements and from the study where the effect of surrounding landscape element on Fe speciation in the stream was studied, according to Wilke *et al., 2001*[97]. The red circles correspond to the areas of the pure 4 or 6 coordinated Fe redox states. For comparison, some model compounds are also added to this pre-edge analysis, i.e. biotite, ferrihydrite, goethite and a 6489 ppm Fe SRN sample at pH 5. This figure is modified from Paper II.

4.2.1 Fe speciation in C2 stream water

The series where Fe-species from different volumes of C2 stream water was adsorbed to a fixed mass of resin resulted in a gradient with respect to Fe adsorption (Figure 6). Adsorption of a smaller volume of stream water sample resulted in a high level of Fe adsorption, whereas adsorption of Fe from larger stream water volumes resulted in lower levels of Fe adsorption. In accordance with the competitive binding experiment with $Fe(C_2O_4)_3^{3-}$ and $Cu(C_2O_4)_2^{2-}$, adsorption of compounds with high binding affinity was favored under conditions when incomplete adsorption of Fe occurred. Adsorption to the positively charged resin is based on electrostatic adsorption and therefore requires negative charges on adsorbing elements. The charge of the compound is likely one important criterion for the observed selectivity (Figures 4 and 6). Binding of 100% Fe from one stream water sample implies that all Fe in that sample is

associated with or comprise of negatively charged compounds, presumably NOM. This is in line with previous studies confirming the existence of Fe(II, III)-NOM complexes and co- precipitates of ferrihydrite and NOM that result when ferrihydrite is precipitated in the presence of NOM[7]. Binding of 100% Fe in this case represents an adsorbed Fe concentration corresponding to ~94µg Fe g^{-1} resin. The corresponding concentration of binding of 28% Fe is 7.5 mg Fe g^{-1} resin. Hence, the concentration of Fe on the resin is significantly lower in the 100% Fe adsorption sample, which generates lower quality XAS spectra compared with samples with higher Fe concentration on the resin. Therefore, there is a tradeoff between representative samples (i.e. high level of Fe adsorption) and quality of the XAS spectra.

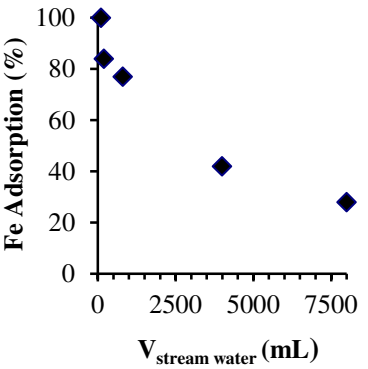

Figure 6. Adsorption of Fe species from C2 stream water to 0.500 g of resin.

XAS analysis of the gradient samples discussed above included WT, XANES, and shell-by-shell EXAFS data fitting (Paper I). The majority of the samples contained features in the WT that could be ascribed to second shell C neighbors (at 2-4 $Å^{-1}$, 2.0-2.4 Å), indicating Fe(II, III)-NOM, and second shell Fe neighbors (at 6-10 $Å^{-1}$, 2.5-3.2 Å), indicating Fe-Fe scattering from precipitated Fe(III) (hydr)oxides (Figure 7). However, variation in the relative intensities and differences in beat patterns, i.e. for features caused by Fe, suggest the existence of several different species (see Figure 7 a, b, d and e). The lack of features caused by second shell Fe in Figure 7c was likely caused by destructive interference (Figure 8). This was confirmed using FEFF calculations on Fe-Fe distances of 3.4 and 3.6 Å respectively. These distances represent the long Fe-Fe distances

obtained for the “high-adsorption” samples (3.6 Å obtained for 100 and 84% Fe adsorption) and “low-adsorption” samples (3.4 Å obtained for 28 and 42% Fe adsorption). The 77% Fe adsorption sample likely contained a mixture of these two endpoints and it was not possible to obtain reasonable shell-by-shell fitting results for this sample.

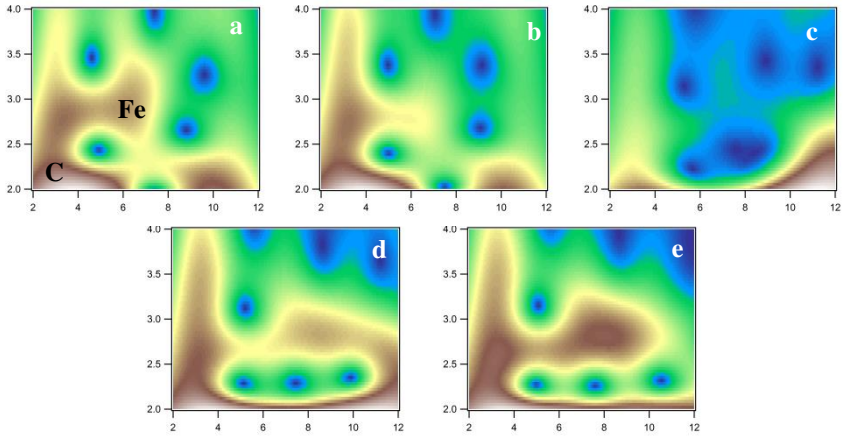

Figure 7. High resolution Morlet WT (η=4, σ=2) for second and third shell backscatters in C2 stream water with a) 100 %, b) 84 %, c) 77 %, d) 42 %, and e) 28 % Fe adsorption. The x-axis is in *k* (Å^{-1}) and y-axis in R (Å). This figure is modified from Paper I.

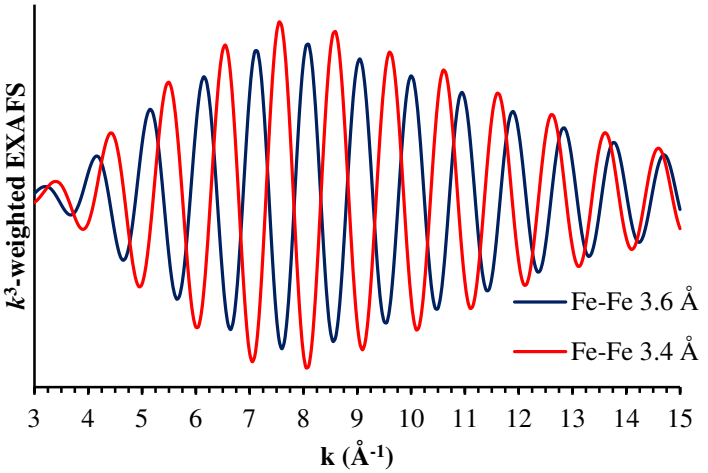

Figure 8. FEFF calculated EXAFS spectra of Fe-Fe paths at 3.4 and 3.6 Å. Modified from Paper I.

The main findings from this study are that there are several different Fe species present in the stream water. Our data suggest the existence of at least two different classes of Fe(II, III)-NOM complexes and at least two different classes of precipitated Fe. The XANES analysis suggested that Fe(III) dominated the Fe speciation, however the 100% Fe adsorption sample probably contained a significant fraction of Fe(II) (Paper I). This was manifested as a shift in the pre-edge. The EXAFS data fitting confirmed the results from the WT through a clear difference between the high-adsorption samples (100 and 84 % adsorption of Fe) compared with the low-adsorption samples (42 and 28% adsorption of Fe). These differences were also clear in the FT, where Fe in the second shell was apparent at longer distances for the high-adsorption samples compared with the low-adsorption samples, see Figure 9. Results from the EXAFS data fitting are presented in Table 2 and Figure 9. For the low-adsorption samples the Fe-Fe distances were present at ca: 3.07 and 3.40 Å, which is in agreement with distances frequently reported for ferrihydrite-like structures[9,109-111]. The Fe-C bond distances for the low-adsorption samples, at 2.83-2.85 Å are in line with previous results presented for five- and six membered chelate rings with carboxylic or hydroxocarboxylic acids[106]. In contrast, the short Fe-C at 2.63-2.66 Å observed for the high-adsorption samples are significantly shorter and more difficult to explain, but short distances have previously been reported for metal-organic complexes[112,113].

The observed differences in Fe-C distances should be interpreted with caution, since they are influenced by short Fe-Fe distances and thus prone to artefacts.

Table 2. Results from k^3-weighted EXAFS data fitting[a] of samples from stream water (C2) collected at the Krycklan Catchment. The table is modified from Paper I (Sundman *et al., 2013*[114])

Sample name (% of adsorbed Fe)	**Path**	**CN**[b]	**R(Å)**	**σ^2(Å^2)**
100	Fe-O	4.0	1.97	0.0055
	Fe-C	2.8	2.66	0.0056[c]
	Fe-Fe	0.5	3.12	0.0100[d]
	Fe-Fe	2.6	3.60	0.0100[d]
	Fe-C-O#	5.6	3.99	0.0112[e]
84	Fe-O	5.0	1.97	0.0069
	Fe-C	2.0	2.63	0.0056[c]
	Fe-Fe	0.7	3.11	0.0100[d]
	Fe-Fe	1.4	3.55	0.0100[d]
	Fe-C-O#	4.0	3.93	0.0112[e]
42	Fe-O	5.9	2.00	0.0079
	Fe-C	1.1	2.85	0.0056[c]
	Fe-Fe	1.4	3.07	0.0100[d]
	Fe-Fe	1.0	3.40	0.0100[d]
	Fe-C-O#	2.2	4.06	0.0112[e]
28	Fe-O	6.0	2.00	0.0086
	Fe-C	0.9	2.83	0.0056[c]
	Fe-Fe	1.4	3.07	0.0100[d]
	Fe-Fe	0.9	3.41	0.0100[d]
	Fe-C-O#	1.8	4.06	0.0112[e]

[a] ΔE_0 was correlated to be identical for all shells. R=bond distance, σ^2=Debye-Waller factor, #=multiple scattering path. S_0^2 was set to 1.0. Uncertainties in CN and R are presented in Paper I.

[b] The multiple Fe-C-O# path was correlated as CN (Fe-C) ×2.

[c] Value adapted from ref[106].

[d] Value adapted from ref[107].

[e] Value correlated according to σ^2 (Fe-C) ×2.

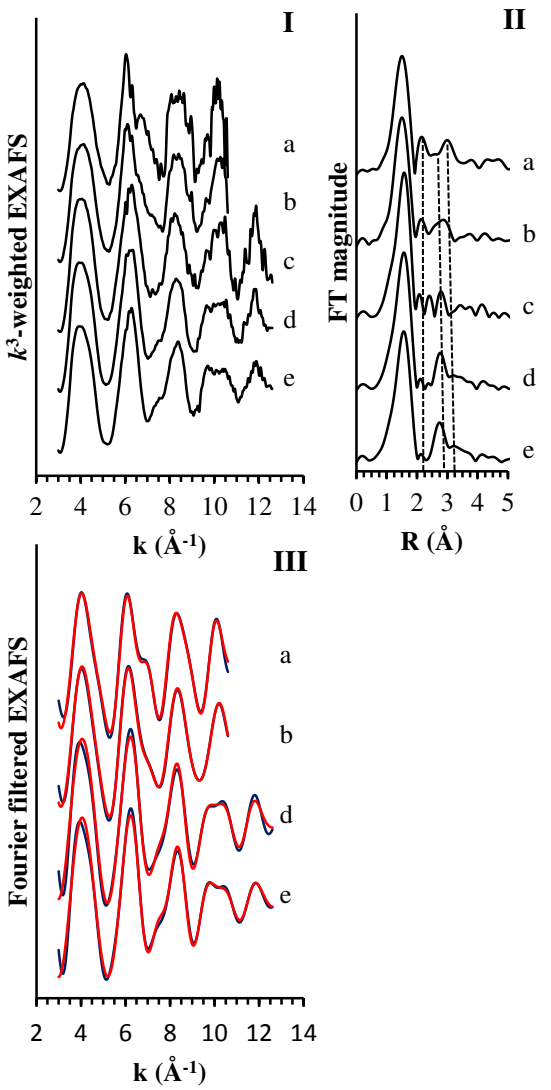

Figure 9. EXAFS data for the C2 stream water samples from the Krycklan catchment according to I) k^3-weighted EXAFS, II) Fourier transformed EXAFS and III) Fourier-filtered EXAFS for a) 100%, b) 84%, c) 77%, d) 42%, and e) 28% adsorbed Fe. For I and II experimental data is shown. For III, blue lines represent experimental data and red lines represent model data. The vertical lines are for visual guidance. The figure is modified from Paper I.

4.2.2 Effect of surrounding landscape

In Paper II, the effect of surrounding landscape on the Fe speciation was studied by comparing 5 different streams, C1-C4 and C10 in Table 1, using the previously described preconcentration protocol. Iron adsorption from the stream waters was incomplete (Paper II). Approximately 88% Fe adsorbed for C2 and 37-56% for the other stream water samples. This was taken into consideration in the comparison between samples. However, since the level of adsorption is similar for all but C2, no major effect of different levels of adsorption is anticipated. This viewpoint is based on the gradient series presented in Paper I which highlighted that the average speciation was very similar within the "high-adsorption" and "low-adsorption" sample groups. The observed differences in the level of adsorption are likely due to differences in concentration and properties of the DOC (e.g. density of functional groups and size).

The pre-edge analysis revealed that all stream water samples contained mixtures of Fe(II) and Fe(III) (Figure 5). All samples have clear contributions from second shell C backscattering in their high resolution WT at 2-4 $Å^{-1}$, 2.0-2.5 Å, representing Fe(II, III)-NOM interactions (Figure 10). Furthermore, they have features at 2-6 $Å^{-1}$, 3.0-4.0 Å caused by C/N/O single and multiple scattering in the second and third shell[8]. According to the WT analysis, the streams from catchments defined as wetland, C3 and C4, (Figure 10 c and d) only contain features caused by Fe(II, III)-NOM interactions. In contrast, the WT for C1 and C2 (i.e. from forest dominated catchments) also contain weak contributions that could be ascribed to Fe backscatters at 9-13 $Å^{-1}$, 2.5-3.0 Å. Finally, the WT for the stream from the mixed catchment (C10, Figure 10e) has a strong contribution from second shell Fe suggesting a high occurrence of precipitated Fe in this sample. Under the studied conditions, the wetland streams (C3 and C4) had lower pH and higher DOC levels compared with the forest streams (C1 and C2), c.f. Table 1. The mixed stream/site had the highest pH and also displayed the strongest contribution from a precipitated Fe phase (Table 1). These results are in agreement with previous studies suggesting pH and NOM to exert strong influence on Fe speciation[8,9].

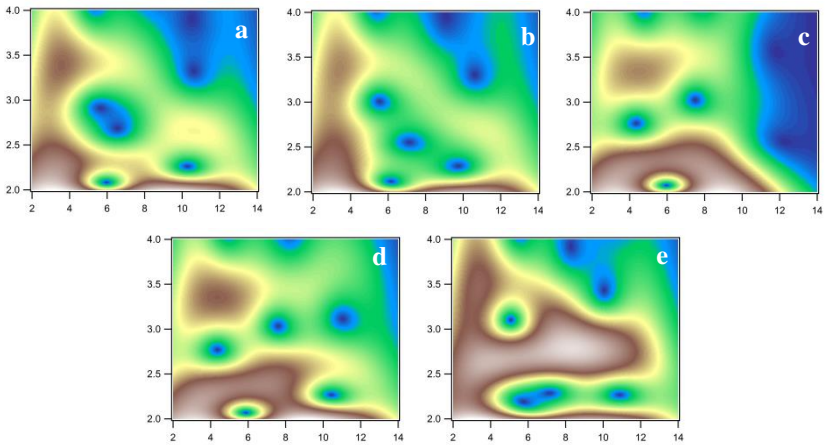

Figure 10. High resolution Morlet wavelet transform (η=10, σ=1) of EXAFS data from Krycklan catchment stream water samples a) C1, b) C2, c) C3, d) C4, and e) C10. The x-axis is *k* ($Å^{-1}$) and the y-axis is R (Å). The figure is modified from Paper II.

The results from the WT analysis were corroborated by the k^3-weighted EXAFS and the corresponding FTs, Figure 11. The samples from the wetland streams (Figure 11 d and e) display beat patterns, in *k*-space, highly similar to $Fe(C_2O_4)_3^{3-}$ (Figure 11 g), confirming the existence of Fe(II, III)-NOM complexes. This was also apparent in the FT (figure 11 d, e and g). Similarly, the second shell FT of ferrihydrite (Figure 11 a) clearly resembles the one of C10 (Figure 11 f). These findings were also supported by the shell-by–shell EXAFS data fitting. All samples were fitted with Fe-C distances of 2.83-2.86 Å (Paper II, ref [115]), which is in accordance with distances reported for chelate ring structures[16,106,116]. The Fe-Fe distances obtained for the forest (C1 and C2) and the mixed (C10) stream water sample suggest a precipitated Fe-phase with a ferrihydrite or goethite like character (Paper II, ref[115]). The low coordination number for the longer distances of the forest samples might also indicate small polynuclear Fe complexes, as suggested by van Genuchten *et al., 2011*[117]. Furthermore, the lack of Fe contributions in the wetland sites suggest the existence of Fe(II)-NOM complexes, as both C3 and C4 contained a significant fraction of Fe(II) according to pre-edge analysis in Figure 5.

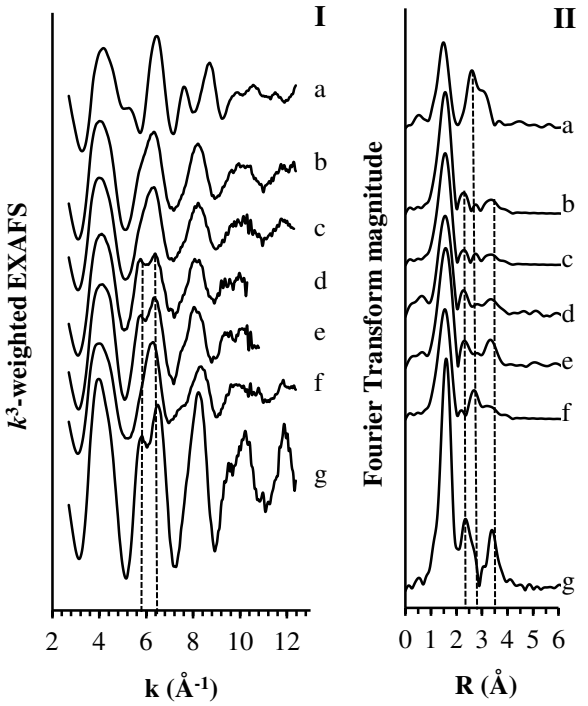

Figure 11. EXAFS data for model compounds (a, g) and stream water samples (b-f) from the Krycklan catchment according to I) k^3-weighted EXAFS and II) Fourier transformed EXAFS for a) ferrihydrite, b) C1, c) C2, d) C3, e) C4, f) C10, and g) $Fe(C_2O_4)_3^{3-}$ solution. The vertical lines are for visual guidance. The figure is modified from Paper II.

4.2.3 Iron speciation within adjacent landscape elements

Iron speciation within adjacent landscape elements included varying amounts of Fe(II, III)-NOM complexes, and in some samples, Fe(III) (hydr)oxides. This variation is attributed to the interactions between Fe and NOM since complexation via NOM suppresses hydrolysis of Fe[8,9]. The results presented within Paper II are in general agreement with those recently presented by Neubauer *et al., 2013*[20]. However, the importance of Fe(II) in these systems was more highlighted in this study (Paper II, ref[115]).

The samples represent the majority of the Fe species present in the solution samples and an inter-sample comparison should not be severely affected by differing extents of adsorption to the resins (Paper II). The pre-edge analysis (Figure 5) revealed that all samples contain a mixture between Fe(II) and Fe(III) and six-coordinated Fe is dominating. The soils show high similarities with the mixed valence Fe(II)/Fe(III) biotite mineral according to XANES analysis of first derivatives (Figure 12 c-f). These findings were further strengthened by the LCF analysis, where all soils were fitted with significant contributions from biotite (Figure 13). For all three soils, the summed fraction for Fe(III)-NOM and biotite was ≥ 0.56 (Paper II). For the soil at 0-10 cm, the fractions represented by biotite and Fe(III)-NOM were almost equal, whereas the fraction represented by Fe(III)-NOM was greater in the soil at 20-30 cm. In contrast, the biotite fraction dominated in the soil at 50-60 cm. The NOM bonded Fe is not necessarily Fe(III) (as discussed above), however, all Fe-NOM model compounds available for the LCF were Fe(III) which is a weakness in our LCF-analysis. These trends were also revealed in the WTs of the soil samples. The features from the soil samples at 0-10 and 50-60 cm are similar to those of ferrihydrite and biotite (Figure 14 a-c and e), whereas the soil at 20-30 cm displayed WT features indicative of Fe(II, III)-NOM contributions (Figure 14 d and k). The k^3-weighted EXAFS and the FT also support these findings. In particular, the spectrum of the 50-60 cm soil is highly similar to the one for the biotite model (Figure 15 b, e).

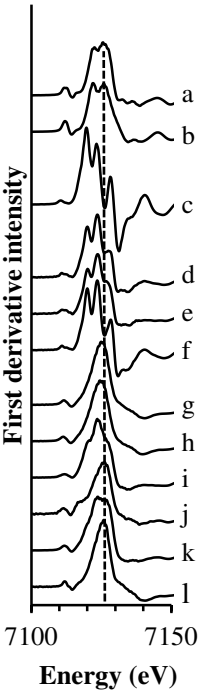

Figure 12. First derivative XANES spectra of samples from various landscape elements of site C2 (d-k) and model compounds (a-c, l) according to: a) goethite, b) 6L-ferrihydrite, c) biotite, d) S4 soil, 0-10 cm, e) S4 soil, 20-30 cm, f) S4 soil, 50-60 cm, g) S4 soil solution, 20-30 cm, h) S4 soil solution, 50-60 cm, i) ground water, j) C2 stream water sample, 82 % adsorbed Fe, k) C2 stream water sample, 28 % adsorbed Fe, and l) 6489 ppm Fe-SRN sample at pH 5. S4 samples are sampled 4m from the C2 stream. The distances refer to distance from the ground level. The dashed lines serve as help to identify changes in peak positions. This figure is modified from Paper II.

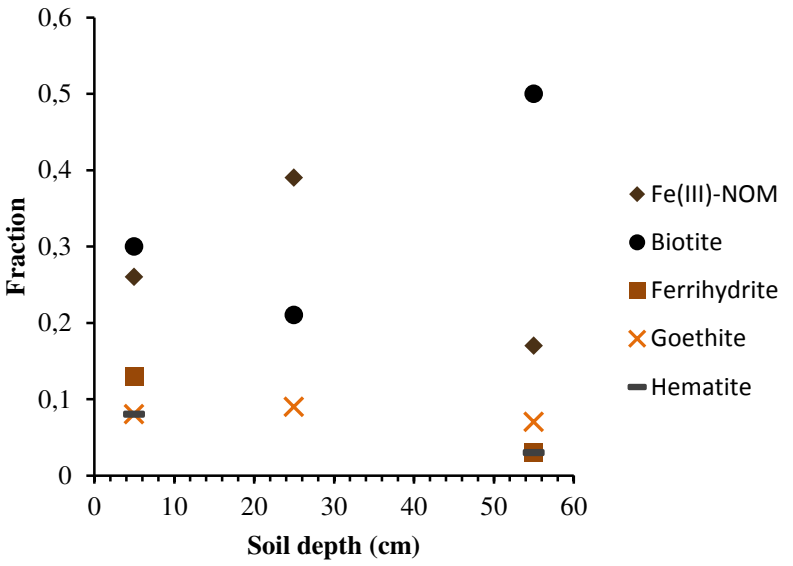

Figure 13. Results from EXAFS LCF for the three soil samples present at 0-10 cm (at 5 cm in the figure), 20-30 cm (at 25 cm in the figure), and 50-60 cm (at 55 cm in the figure).

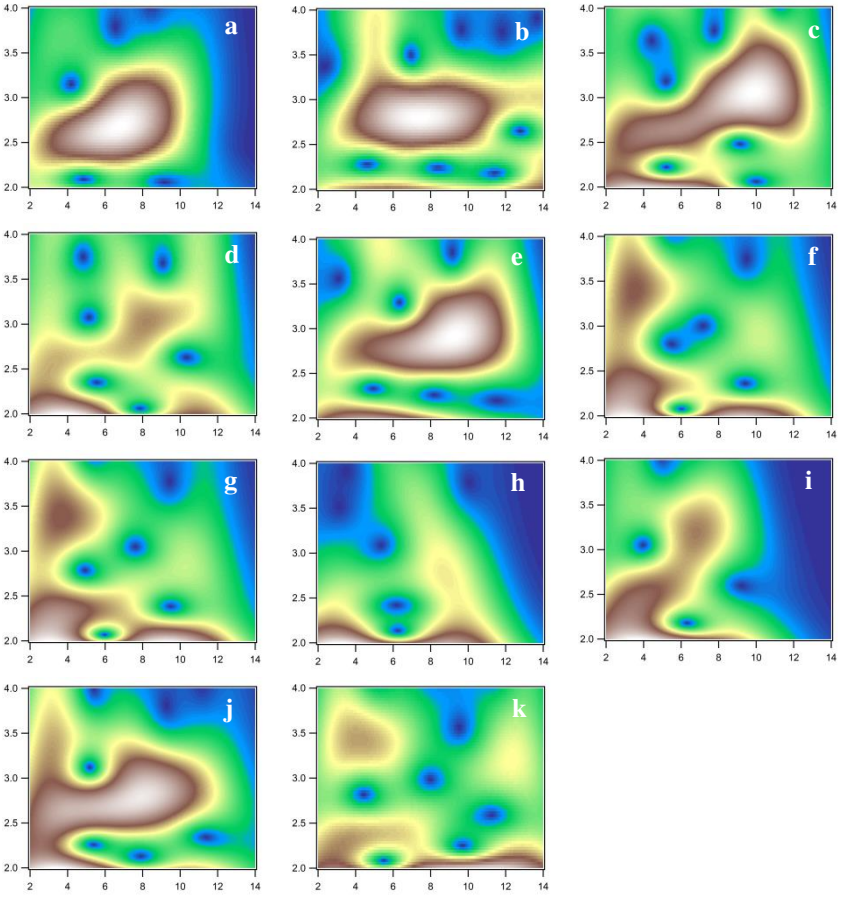

Figure 14. High-resolution Morlet wavelet transforms (η=10, σ=1) of EXAFS data collected on samples from various landscape elements of site C2 (c-j) and model compounds (a,b and k) according to a) 6-line ferrihydrite, b) biotite, c) S4 soil, 0-10 cm, d) S4 soil, 20-30 cm, e) S4 soil, 50-60 cm, f) S4 soil solution, 20-30cm, g) S4 soil solution, 50-60 cm, h) groundwater, i) C2 stream water with 82% adsorbed Fe, j) C2 stream water with 28% adsorbed Fe, and k) 6489 ppm Fe-SRN at pH 5. S4 samples are sampled 4m from the C2 stream. The distances refer to distance from the ground level. The x-axis is *k* ($Å^{-1}$) and the y-axis is R (Å). This figure is modified from Paper II.

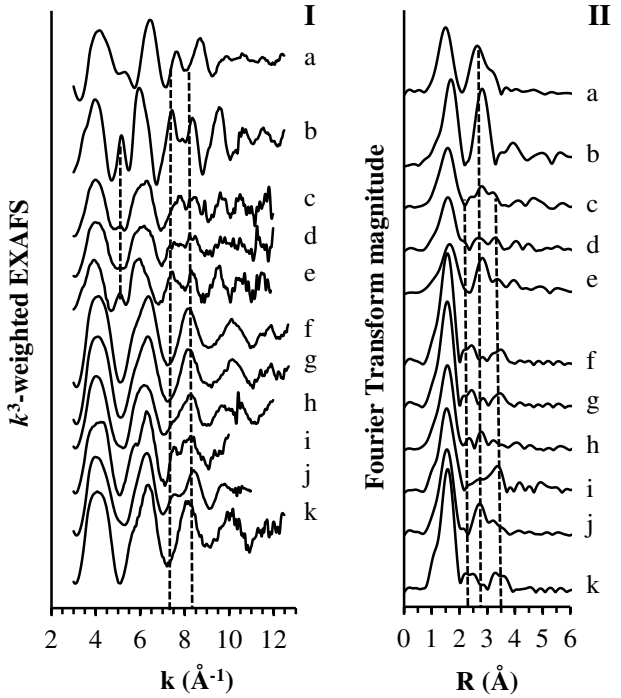

Figure 15. k^3-weighted EXAFS spectra I) and corresponding Fourier transforms (II) of the samples from the various landscape elements of site C2 (b-j) and model compounds (a,k) according to a) 6L-ferrihydrite, b) biotite, c) S4 soil, 0-10cm, d) S4 soil 20-30 cm, e) S4 soil, 50-60 cm, f) S4 soil solution, 20-30 cm, g) S4 soil solution, 50-60 cm, h) ground water, i) C2 stream water, 82 % adsorbed Fe, j) C2 stream water, 28 % adsorbed Fe, and k) 6489 ppm Fe-SRN at pH 5. S4 samples are sampled 4 m from the C2 stream. The distances refer to distance from the ground level. The dashed lines serve as help to identify changes in peak position. This figure is modified from Paper II.

The soil solutions contained more Fe(II) than their parent soils (Figure 5), which suggests enrichment processes, e.g. microbial reduction[28]. Furthermore, the combined results from the XANES analysis (Figure 12), the WT (Figure 14) and the shell-by-shell EXAFS data fitting (Paper II) suggest the existence of only Fe(II, III)-NOM complexes in the soil solutions. This has several implications: most importantly, the observed high levels of Fe(II) are thus likely to be Fe(II)-NOM complexes. In addition, the NOM present in the soil solutions must contain functional

groups that form complexes with Fe that are strong enough to suppress Fe(II) oxidation. In contrast, both the groundwater and the stream water samples contain significant fractions of precipitated Fe, as indicated in the WT (Figure 14 h-j). This suggests that there might be Fe(II) oxidation and/or Fe(III) precipitation in the groundwater caused by e.g. oxygen. This is also confirmed in the pre-edge analysis, which suggests that the groundwater contains less Fe(II) than the soil solutions (Figure 5). However, the WTs and the EXAFS data (Figure 14 and 15) show clear evidence for Fe(II, III)-NOM complexes in both the groundwater and the stream water samples. Hence, they contain a mixture between organically complexed Fe and precipitated Fe(III). The stream water samples contained more Fe(II) than the groundwater, which indicates an inflow of Fe(II). The fate of Fe(II) in the stream is then determined by present conditions, e.g. properties of NOM and/or oxidizing conditions. Furthermore, the stream water sample with 82 % adsorbed Fe is indicated to contain more Fe(II) compared with the sample where only 28 % Fe was adsorbed. This is in line with the results from the gradient samples, where the sample where 100% of the Fe was adsorbed contained the largest contribution of Fe(II). This indicates that Fe(II) complexes/compounds have a lower affinity for binding to the resin compared with Fe(III). The underlying mechanism for this observation is difficult to assess, since these samples contain mixtures of organically complexed Fe and precipitated Fe.

4.2.4 Reactivity of Fe from a natural stream water towards As(V)

In accordance with the previous studies of Fe speciation in stream water from the C2 site, in Paper I and II, the native stream water sample contained both Fe(II, III)-NOM complexes and precipitated Fe(III) (hydr)oxides (Paper III). However, addition of As(V) to this natural stream water changed Fe speciation. This was manifested as a decrease in the contributions from corner- and edge sharing Fe and Fe-C interactions. Adsorption of As(V) to the surface of Fe(III) (hydr)oxides or formation of ternary As(V)-Fe(II, III)-NOM complexes do not induce structural changes in the solid Fe phase or change the Fe(II, III)-NOM complexes. Therefore the observed changes in Fe speciation together with the presence of Fe-As interactions indicate the formation of new Fe and As bearing phases. Furthermore, the co-occurrence of aqueous As(V) and Fe(II, III)-NOM complexes suggests that the Fe(II, III)-NOM complexes were strong enough to make a fraction of Fe non-reactive towards As(V).

Around 65% of Fe and 85-100% of As in the stream waters were adsorbed to the resins (Paper III). The high level of As adsorption may be attributed to the anionic character of the arsenate as this would favor binding to the positively charged TMA-groups on the resins. Arsenic XANES analysis confirmed the conservation of the valence of As(V) and indicated that aqueous $H_2AsO_4^-$ constituted a significant fraction of the As species in these samples. Similarly, Fe XANES analysis indicated that Fe(III) was the dominant oxidation state for Fe and the ferrihydrite-like structure of the first derivative XANES indicated that Fe(III) (hydr)oxides were common. These findings were corroborated by the WT analysis. The As WTs of the spiked stream water samples (Figure 16c-e) were similar and displayed a maximum at ca. 6 $Å^{-1}$, 2.5 Å, which is caused by Fe backscattering (Paper IV). The shape of this feature resembles the elongated shape of $FeAsO_4$(s) (Figure 16b), rather than that of arsenate adsorbed onto goethite where the WT features are shifted towards higher *k*-values (Figure 16a). This indicates that Fe backscattering in these samples is likely to be caused by $FeAsO_4$(s). Increasing levels of As(V) addition resulted in an increased intensity of features at ca: 3 $Å^{-1}$, 2.5 Å and 3 $Å^{-1}$, 3.8 Å similar to those of aqueous arsenate (Figure 16f). These features are caused by multiple scattering within the arsenate tetrahedron[46]. A likely cause of this trend is adsorption of aqueous arsenate by the resins. The Fe WTs of the samples (Figure 16i-k) displayed a high intensity region at 2-4 $Å^{-1}$, 2-2.5 Å which is caused by Fe-C single scattering from organically complexed Fe (Figure 16l)[8,9,16]. In addition, the native C2 stream water sample and the C2 stream water sample with added As(V), to a Fe/As ratio of 3.7, contained high intensity regions at 5-6 $Å^{-1}$, 2.5-3 Å caused by Fe-Fe single scattering (Figure 16g, j and k). In contrast, the sample with the highest level of As concentration did not display features caused by Fe or As backscattering (Figure 16h and i). This trend with decreasing/non-existing Fe/As backscattering is likely caused by destructive interference between the Fe-As path at 3.30 Å and Fe-Fe paths at 3.10 and 3.60 Å as outlined in Paper IV.

These results were corroborated by the shell-by-shell As and Fe EXAFS data fitting (Paper III). The coordination number of the As-Fe path in the As-EXAFS decreased with increasing As concentrations. This is in line with an increased concentration of free arsenate binding to the resin, as this lowers the average As-Fe interaction. Fe EXAFS fitting results indicated the presence of two pools of Fe: organically complexed Fe and Fe(III) (hydr)oxides. Increasing As concentrations decreased the

contributions of edge- and corner-sharing Fe, but increased Fe-As interactions. The collective results from this study thus indicates that the Fe(II, III)-NOM and Fe(III) (hydr)oxides initially present in the stream water underwent a phase transformation to an $FeAsO_4$(s) phase upon addition of arsenate. Furthermore, the concurrent existence of aqueous arsenate and Fe(II, III)-NOM complexes indicate that the complexes were sufficiently strong to make a fraction of the Fe non-reactive towards As(V). Natural stream waters contain many different elements that may interact with As, e.g. Al. However, the low Al concentration in these stream water samples suggests that As-Al interactions were of minor importance in this particular study.

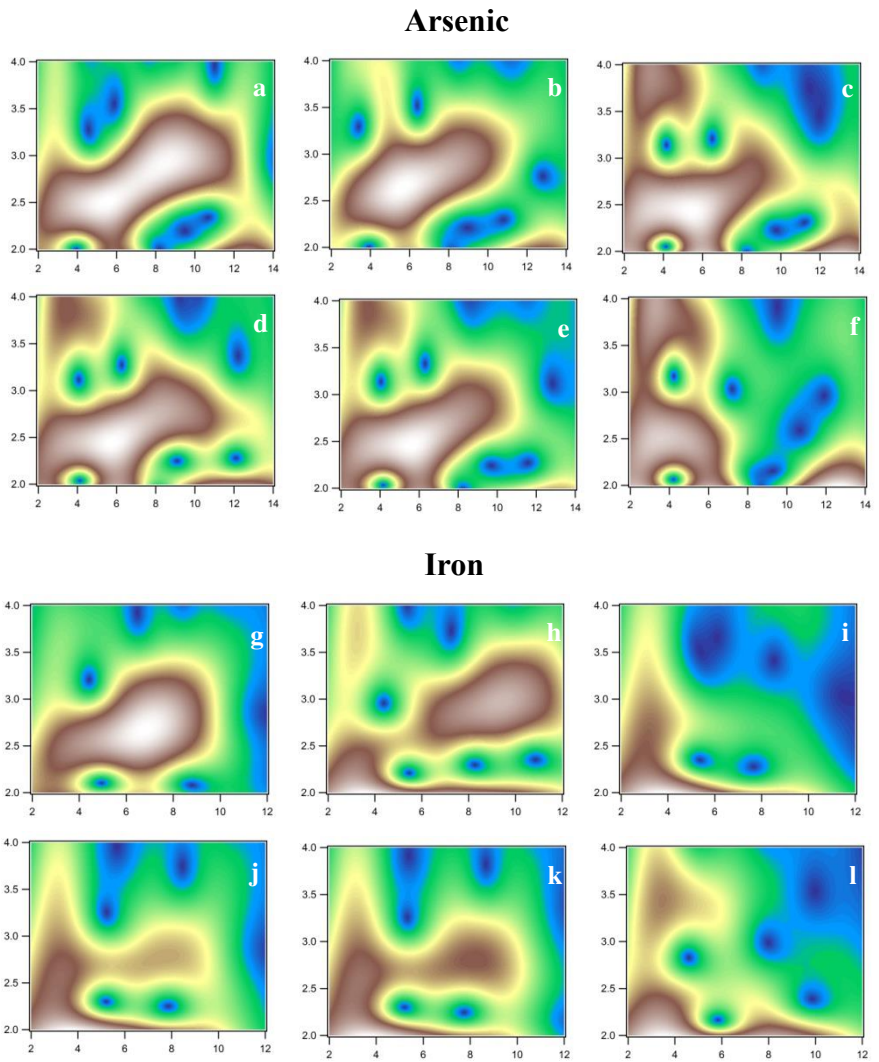

Figure 16. High resolution As-WT modulus of second and third coordination shells (η=4, σ=2) for k^3-weighted EXAFS spectra of a) 1.8µmol/m² arsenate adsorbed on goethite at pH 5.3[46], b) amorphous $FeAsO_4$(s), c) C2, with 51.9% As relative to [Fe], d) C2, with 27.7% As relative to [Fe], e) C2, with 7.7% As relative to [Fe], f) 150mM $HAsO_4^{2-}$ solution[46], and Fe-WT modulus of second and third coordination shells (η=4, σ=2) for g) 6L ferrihydrite[9], h) amorphous $FeAsO_4$(s), i) C2, with 51.9% As relative to [Fe], j) C2, with 7.7% As relative to [Fe], k) native C2 sample and l) 6489 ppm Fe SRN sample at pH 5[9]. The x-axis is k (Å^{-1}) and the y-axis is R (Å).This figure is modified from Paper III.

4.3 Studies of ternary As(V)/P(V)-Fe(III)-NOM systems

The studies of the ternary As(V) or P(V)-Fe(III)-NOM systems in Papers IV and V revealed a strong dependence between total concentrations and the speciation of As, Fe and P. The main constituents in these samples were Fe(III)-NOM complexes, precipitated Fe(III) (hydr)oxides, $FeAsO_4$(s), $FePO_4$(s), solid solutions of ferrihydrite with arsenate or phosphate incorporated in the bulk, and aqueous arsenate and phosphate. At low concentrations, complexation between Fe(III) and NOM suppressed Fe hydrolysis, which resulted in Fe(III)-NOM complexes and free arsenate or phosphate. At higher concentrations, both Fe(III)-NOM complexes, $FeAsO_4$(s) or $FePO_4$(s) and/or polymeric Fe precipitated. A fraction of the Fe(III) was non-reactive towards As(V) and P(V) due to the formation of stable Fe(III)-NOM complexes. Chemical equilibrium models were able to explain the trends observed in EXAFS and IR data without including surface complexation or formation of ternary As(V)/P(V)-Fe(III)-NOM complexes.

In Paper IV two ternary As(V)-Fe(III)-NOM systems were presented, one with NOM=SRFA and one with NOM=SRN. Although SRFA only constitute a minor fraction of the SRN both materials displayed the same trends. In Paper V the ternary P(V)-Fe(III)-SRN system was studied and it was in general agreement with the findings in Paper IV. In addition, ternary systems with As(V) or P(V) and Fe(III) added to a peat humic acid (PPHA=NOM) have also been investigated. They also displayed the same general trends as those with other sources for the NOM. Since the same trends were observed irrespective of source of NOM and the presence of As(V) or P(V) the results from Papers IV and V will be presented using representative samples from the different series.

4.3.1 Binary Fe(III)-NOM systems

The reference binary systems, Fe(III)-PPHA and Fe(III)-SRN are already published[8,9]. The corresponding Fe(III)-SRFA binary reference system is presented in Paper IV and is highly similar to those of PPHA and SRN. Briefly, the Fe speciation in the presence of NOM is determined by pH and Fe concentration. Low pH and low concentrations favor formation of Fe(III)-NOM complexes, whereas Fe(III) (hydr)oxides precipitates at higher pH and/or concentrations. For Fe(III)-SRN and Fe(III)-SRFA in

Paper IV, two simple models for the Fe-NOM complexes were obtained based on XAS and IR spectroscopic observations. The complexes were assumed to have 1:1 stoichiometry and chelate structure with carboxyl functional groups. Two complexes (Fe(III)-NOMH$_{-1}$ and Fe(III)-NOMH$^{-}_{-2}$, where NOM= SRFA or SRN) were needed in order to simulate the observed Fe(III)-NOM complex formation. These differed in their degree of deprotonation. The stability constants obtained for SRFA and SRN were similar, which is in line with the EXAFS results. To illustrate speciation in the binary Fe(III)-SRN system a distribution diagram was constructed, cf. Figure 17. Fe(III)-NOM complexes dominated at low pH, but increasing pH results in the formation of a solid Fe(III) phase (Figure 17).

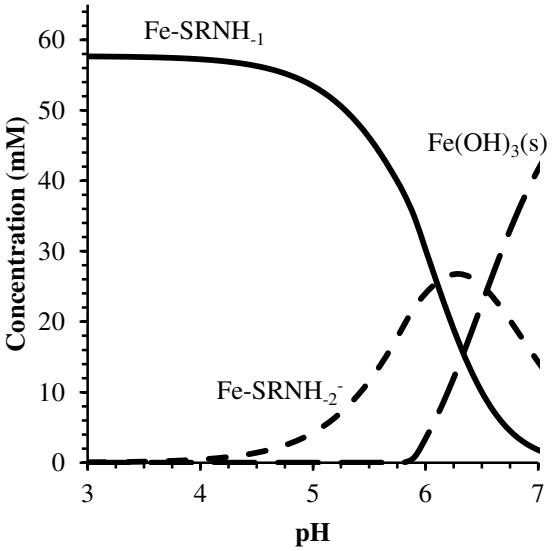

Figure 17. Distribution diagram for 57 mM Fe(III) and 68 mM dicarboxylic acid groups from the active fraction of carboxylic acid groups in SRN.

4.3.2 IR spectroscopic results in the ternary systems

In the ternary systems, the focus of the IR spectroscopy studies was the arsenate and phosphate vibrations at 950-700, and 1200-850 cm^{-1}, respectively (Figure 18 I and II). These were studied for the 22 916-22 918 ppm Fe(III) SRN samples with Fe/As and Fe/P ratios of 1 at pH 3.0-6.5. The spectra contained several peaks; peaks caused by the organic

material (SRN), peaks characteristic of aqueous arsenate and phosphate and broad peaks at 810, and 1046 cm^{-1}, respectively (Figure 18 I, II, Papers IV and V). The broad peaks were caused by $FeAsO_4(s)$ and $FePO_4(s)$ (Figure 18b and g). No peaks characteristic of arsenate or phosphate adsorbed to the surface of Fe(III) (hydr)oxides were present in the spectra (Figure 18h, Papers IV and V), indicating that the two main As and P species were the $FeAsO_4(s)$, $FePO_4(s)$ and aqueous arsenate and phosphate, respectively. The aqueous concentrations ranged 20-35, and 12-20 % respectively, see Figure 18 III. This indicates that at As/Fe=1 or P/Fe=1, a fraction of the Fe(III) is not accessible for reaction with As(V) or P(V). Both As(V) and P(V) displayed a weak minimum in their bound fractions around pH 5 (Figure 18 III). The overlaps between aqueous $H_2PO_4^-$ and $FePO_4(s)$ in the phosphate samples made quantification of aqueous $H_2PO_4^-$ more complicated than the corresponding quantification of aqueous $H_2AsO_4^-$. Therefore, the $H_2PO_4^-$ concentrations are associated with larger uncertainties. As a consequence, the bound fractions of As(V) and P(V) in Figure 18 III are considered to be in the same range. Finally, increasing Fe/As ratio in Paper IV resulted in an increase of bound As(V) which indicates that a fraction of Fe(III) is non-reactive towards As(V) due to Fe(III)-NOM complex formation.

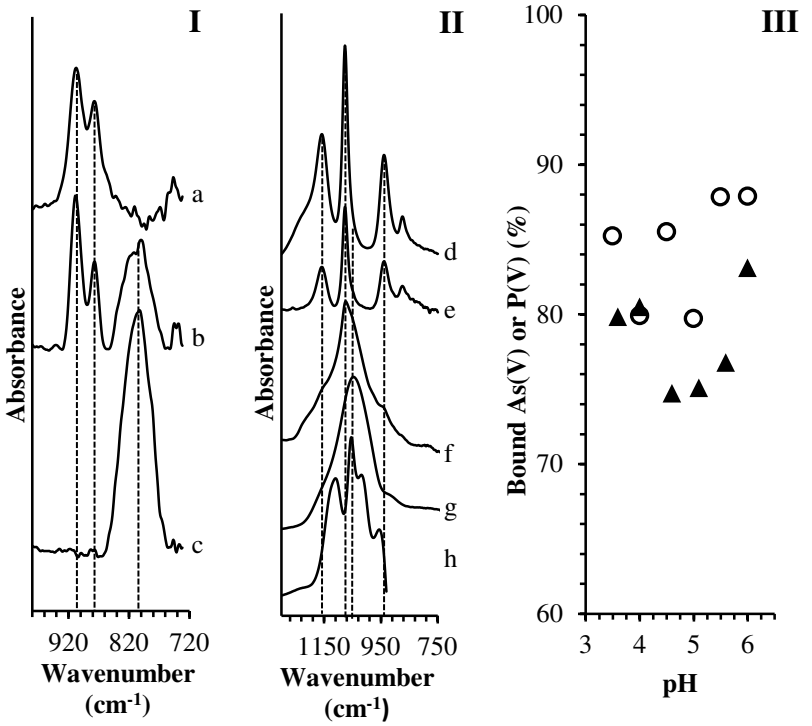

Figure 18. IR spectra of I) a) aqueous $H_2AsO_4^-$, b) SRN sample at pH 4.6 with 22 916 ppm Fe(III) and Fe/As=1, c) amorphous $FeAsO_4$(s), II) d) aqueous $H_2PO_4^-$, e) SRN sample at pH 4.1 with 22 918 ppm Fe(III) and Fe/P=1 and spectral contributions from SRN and $FePO_4$(s) subtracted, f) SRN sample at pH 4.1 with 22 918 ppm Fe(III) and Fe/P=1 and spectral contributions from SRN subtracted, g) amorphous $FePO_4$(s) and h) 2.2 µmol/m² $H_2PO_4^-$ adsorbed on goethite at pH 5.2, and III) estimated bound concentrations (in %) of arsenate (black triangles) and phosphate (open circles). The vertical dashed lines are for visual guidance.

4.3.3 XANES and WT analysis of the ternary systems

The Fe XANES analysis captured the concentration dependent behavior of the ternary systems: at low concentration the first derivative XANES displayed a broad and quite featureless peak, similar to that of a Fe(III)-NOM reference solution (Figure 19a, f), however increasing concentration resulted in the development of more peaks, indicative of $FeAsO_4$(s) or $FePO_4$(s) (Figure 19d, and j, respectively). It was possible to resolve ferrihydrite and $FeAsO_4$(s) or $FePO_4$(s) based on the peak positions

(Figure 19d, e, j and k). Furthermore, the XANES analysis confirmed the conservation of the As(V) and Fe(III) oxidation states (Papers IV and V).

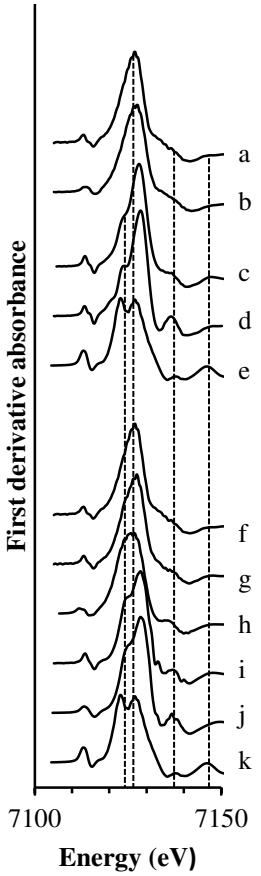

Figure 19. First derivative Fe XANES of SRN samples at pH 5.0-5.3 (a-c, f-i) and reference compounds (d-e, j-k) according to a) 6489 ppm Fe(III), b) 6485 ppm Fe(III) and Fe/As=1.2, c) 22 916 ppm Fe(III) and Fe/As=1, d) amorphous $FeAsO_4$(s), e) 6L-ferrihydrite, f) 6489 ppm Fe(III), g) 5000 ppm Fe(III) and Fe/P=1.2, h) 22 916 ppm Fe/P=1.1, i) 50 000 ppm Fe(III) and Fe/P=1, j) amorphous $FePO_4$(s), and k) 6L-ferrihydrite. The vertical dashed lines are for visual guidance.

The concentration dependence was also revealed in the WT analysis, e.g. increasing concentrations decreased the As WT features caused by aqueous arsenate (Figure 20a, g-i) and increased WT features caused by As-Fe backscattering. In addition, the As WT showed increased contributions from As-Fe single scattering at increased Fe/As ratio (Figure 20j-l). In accordance with the study where arsenate had been added to natural stream water, the WTs contained high intensity regions indicative of As-Fe single scattering (8 $Å^{-1}$, 3 Å) and features caused by scattering within the arsenate tetrahedron (3 $Å^{-1}$, 2.5 Å and 3 $Å^{-1}$, 3.8Å). The shape of the As-Fe single scattering feature is more in agreement with an amorphous $FeAsO_4$(s) phase, than with arsenate adsorbed to the surface of an iron mineral as this would shift the center of gravity towards higher *k*-values. The As WT thus supported the finding from the IR spectroscopy studies, that some arsenate remain free in solution which indicates that a fraction of Fe(III) is non-reactive towards As(V). Finally, a pH trend was also observed: increasing pH increased WT features caused by scattering within the arsenate tetrahedron (Figure 20d-f) which suggests that the concentration of free arsenate increases as a function of pH within the studied pH interval. Observing trends from the Fe WT was more complicated due to the co-occurring features from Fe(III)-NOM and Fe(III) (hydr)oxide. For the ternary As(V)-Fe(III)-NOM system, destructive interference between the Fe-As path and long and short Fe-Fe paths complicated the analysis (Paper IV). For the ternary P(V)-Fe(III)-SRN system, there was an overlap between the Fe-C and Fe-P single scattering (Paper V). However, the elongated shape of the Fe-P features enabled its identification at higher concentrations (Paper V).

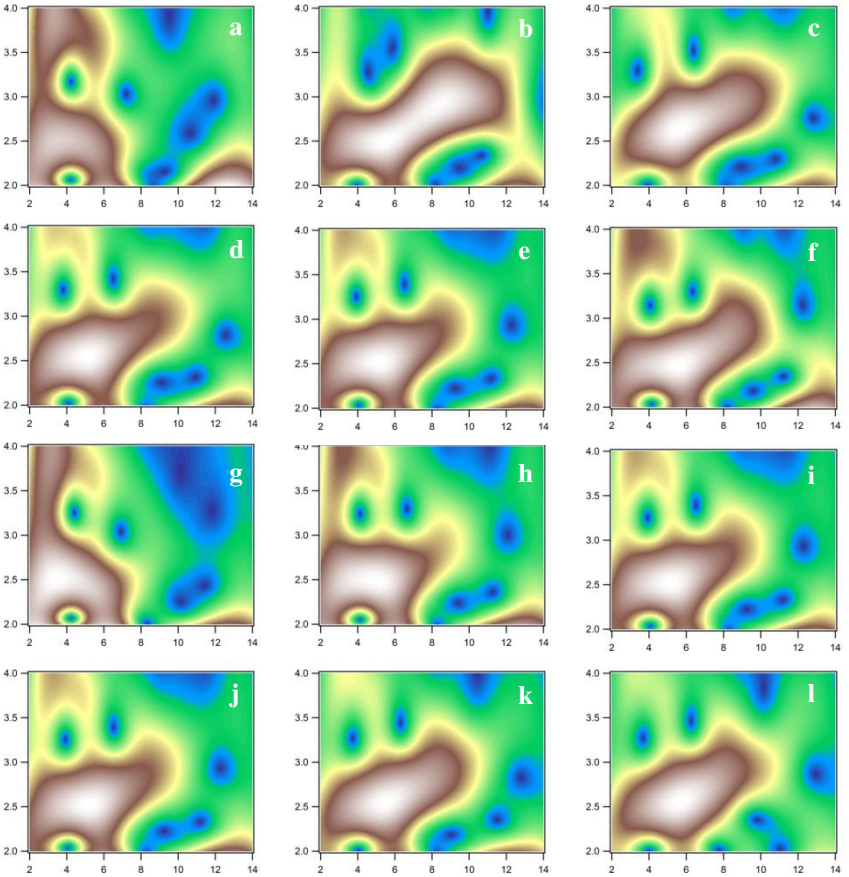

Figure 20. High resolution As-WT modulus of second and third coordination shells (η=4, σ=2) for k^3-weighted EXAFS spectra of reference compounds (a-c) and spectra displaying the effect of pH in 26 945 ppm Fe SRFA-samples at pH 3.0, 5.1 and 6.5 respectively (d-f), effect of concentration at pH 5 (g-i) and effect of Fe(III) to As(V) ratio in SRFA with 26 945 ppm Fe at pH 5.1 (j-l) according to a) 150 mM $HAsO_4^{2-}$ solution, b) 1.8 µmol/m² arsenate adsorbed on goethite at pH 5.3, c) amorphous $FeAsO_4$(s), d) SRFA4, e) SRFA5, f) SRFA6, g) 6736 ppm Fe (SRFA1), h) 13 473 ppm Fe (SRFA3), i) 26 945ppm Fe (SRFA5), j) Fe(III)/As(V) ratio 1.0 (SRFA5), k) Fe(III)/As(V) ratio 4.0 (SRFA7), and l) Fe(III)/As(V) ratio 20.0 (SRFA 8). The x-axis is *k* (Å^{-1}) and the y-axis is R (Å). This figure is adapted from Paper IV.

4.3.4 EXAFS results for the ternary systems

The quantitative EXAFS data fitting also reflected the strong linkage between As, Fe and P speciation and concentration, pH and Fe/As or Fe/P ratio. At low concentrations, e.g. 7043 ppm Fe with Fe/P=1 or 16 mM Fe(III) and P(V), the spectra of P(V)-Fe(III)-PPHA and Fe(III)-PPHA at the same pH are almost identical, c.f. Figure 21a, b. Under these conditions, NOM represented by PPHA, SRFA or SRN complex the majority of the Fe(III) and only minor fractions of Fe(III) may precipitate in the form of $FePO_4$(s) or other P(V)-bearing Fe-phases (Papers IV and V). Thus, most As(V) or P(V) remain in solution under those conditions. Even at high concentrations, i.e. 67 243 ppm or 66.7 mM Fe(III) in SRFA at pH 5.3, contributions from both Fe(III)-NOM complexes, polymeric Fe and Fe-As interactions are identified in the WTs and shell-by-shell data fitting (Paper IV). Hence, the Fe(III)-NOM complexes are strong and play an active role over a wide range of concentrations. Previous studies have also shown that they play an important role over the whole studied pH interval, pH 3-7[8,9].

The As and Fe EXAFS data presented in Paper IV indicated that at least two As(V)-containing solid phases ($FeAsO_4$(s) and $Fe(OH)_{1.5}(AsO_4)_{0.5}$(s)) are formed in these systems. Briefly, Fe-As interactions detected at high total concentrations and high pH are unlikely to be caused by $FeAsO_4$(s), since $FeAsO_4$(s) mostly forms under more acidic conditions. Furthermore, given the low Fe/As ratio, there are not enough surface sites at the Fe minerals to adsorb these quantities of As(V). Rather, formation of a solid solution, where As(V) exists in the ferrihydrite bulk, in accordance with Thibault *et al.*, 2009[90], is likely to account for these observations. In the ternary P(V)-Fe(III)-SRN system presented in Paper V, the corresponding $FePO_4$(s) and solid solution, $Fe(OH)_3(PO_4)_{0.5}$(s) are suggested to form. As already discussed, increasing total concentrations lowers the fraction of Fe(III)-NOM formed and increases precipitates of $FePO_4$ and/or polymerized Fe(III) (hydr)oxides, e.g. ferrihydrite (Figure 21c, d). $FeAsO_4$(s) and $FePO_4$(s) dominate at low pH and polymerized Fe dominates at higher pH. This trend was simulated with the chemical equilibrium model developed in Paper IV, c.f. Figure 22. The distribution diagram in Figure 22 also displays another trend; increasing Fe/As ratios reduces the concentration of arsenate in solution since this favors formation of As(V) bearing solids. This is also in line with the previous results from the IR and WT analysis suggestion that a fraction of Fe(III) is

non-reactive towards As(V) and P(V) due to stable Fe(III)-NOM complexes.

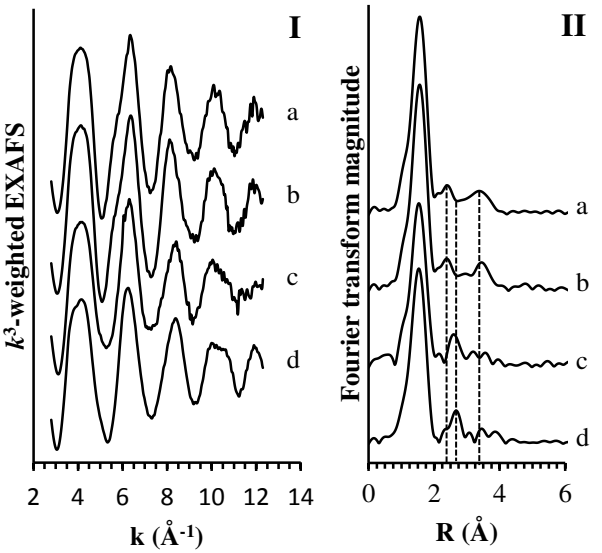

Figure 21. k^3-weighted EXAFS spectra I) and corresponding Fourier transforms II) of a) PPHA sample at pH 5.1 with 5100 ppm Fe(III), b) PPHA sample at pH 5.3 with 7043 ppm Fe(III) and 5869 ppm P(V), c) PPHA sample at pH 5.7 with 57 402 ppm Fe(III) and P(V), and d) amorphous $FePO_4$(s).

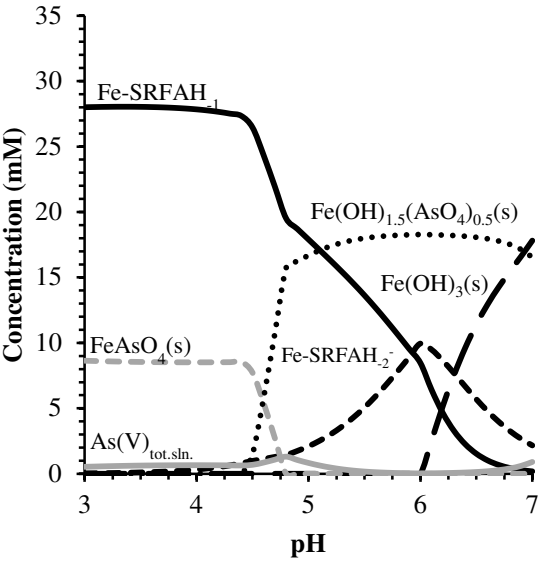

Figure 22. Distribution diagram for 36.7 mM Fe(III), 9.0 mM As(V) and 38 mM dicarboxylic acid groups from the active fraction of carboxylic acid groups in SRFA. Fe-SRFAH$_{-1}$ and Fe-SRFAH$^{-}_{-2}$ represent the two Fe(III)-NOM complexes in this model, As(V)$_{tot.\ sln}$ is total As(V) concentration in solution, Fe(OH)$_3$(s) represent ferrihydrite and Fe(OH)$_{1.5}$(AsO$_4$)$_{0.5}$(s) is the solid solution where As(V) is incorporated into the bulk of ferrihydrite.

5. Summary and future work

This thesis focuses on the importance of NOM in the speciation of Fe, which affects numerous biogeochemical cycles. Fe(II, III)-NOM complexes were identified in both natural systems and in the SRFA, SRN and PPHA samples. As previously stated, Fe complexation with NOM suppresses Fe hydrolysis[9] and thus limits Fe(III) (co)precipitation and the amount of surface sites available for binding of other elements. Fe(III) (hydr)oxides, FeAsO$_4$(s), FePO$_4$(s) and/or mixed Fe(III)/As(V) or Fe(III)/P(V) solid phases were primarily identified in samples with higher pH and/or high concentrations of As(V), Fe(III) and P(V). The results discussed herein have provided a protocol that enables studies of dilute elements in liquid samples, new knowledge regarding Fe speciation and reactivity in natural systems, knowledge about complexation and

precipitation processes in ternary As(V)/P(V)-Fe(III)-NOM systems, but they also highlight current knowledge gaps that limits our interpretations.

5.1 Possibilities with the preconcentration protocol

The preconcentration protocol based on ion exchange resins was developed for studies of Fe speciation in dilute natural waters. However, since the method is based on the driving force of electrostatics, it can be applied to a wide range of different elements, samples, studies and used in combination with other methods. For example, our group has recently used this protocol to probe P speciation in stream waters via NMR and for Al-XANES studies of stream water samples. Speciation studies in lakes have been conducted using a similar method[23]. The construction of the Fe gradient series with C2 stream water highlighted another possibility with this protocol; it enables differentiation between species with different properties present in the same sample. Furthermore, using a combination of several techniques, for example size fractionation, isotope studies and separation in a gradient via the ion exchange protocol can be a fruitful approach for determination of the fate of e.g. Fe in a stream or river water.

5.2 Fe speciation in Krycklan Catchment

Regarding Papers I-III, these studies represent snap shots of Fe speciation, in a limited number of sites from the Krycklan Catchment, during low-flow conditions in autumn and early winter. They highlight the diversity in Fe speciation; the gradient series from the forested C2 site did not only reveal the existence of two pools of Fe; Fe(II, III)-NOM and precipitated Fe(III) (hydr)oxides, but it also provided evidence for the existence of several subspecies within those two groups. In contrast, the organic rich soil solutions and stream water from wetland sites (C3 and C4) only contained Fe(II, III)-NOM complexes.

5.2.1 Geochemical significance of Fe(II, III)-NOM complexes

Given the different reactivity of Fe(II, III)-NOM complexes and precipitated Fe(III) (hydr)oxides, studies of Fe speciation over longer time periods could, for example, improve our understanding of contaminant transport. More specifically, how would DOC dilution observed in C4 during spring flood affect Fe-speciation since all Fe appears to be bound

by NOM under the base-flow conditions? Similarly, how would the enhanced DOC concentrations in C2 (during spring flood) be reflected in the distribution between Fe(II, III)-NOM-complexes and precipitated Fe phases? As these questions are strongly linked to properties of the DOC (i.e. its complexation properties) concurrent studies of DOC properties can be beneficial.

Complexation of Fe via NOM protects Fe from forming Fe minerals or co-precipitates with other elements. Therefore, it is of geochemical significance for other elements, e.g. As(V), if there is a change in the strength or occurrence of Fe(II, III)-NOM complexes as this will affect the bioavailability of As(V). Spiking stream waters from the wetland sites, that are likely to only contain Fe(II, III)-NOM-complexes, with As(V) would reveal if the complexes are sufficiently strong to suppress precipitation of $FeAsO_4$(s). Combined As- and Fe-XAS studies can conclude whether As(V) interacts with Fe (via $FeAsO_4$(s) co-precipitates, in a mixed phase or as a surface complex adsorbed to an Fe mineral surface) and if Fe speciation is intact, i.e. Fe(II, III)-NOM complexes only or if the addition of As(V) result in the formation of new Fe phases.

Given the relatively high Fe(II) concentrations found in the natural stream water and soil solution samples (Paper II), further characterization of Fe(II)-NOM interactions is motivated. Since Fe(III) speciation in the presence of NOM is highly influenced by pH and total concentration[8,9], an initial approach for characterization of Fe(II)-NOM complexes could be conducted with emphasis on those two parameters. Furthermore, the stream waters are supposed to be well aerated, and this indicates that the Fe(II)-NOM complexes are very stable under the studied conditions. Oxidation of Fe(II) to Fe(III) via molecular O_2 is well known, therefore the strengths or stabilities of the complexes under oxic, partly anoxic and anoxic conditions may be of environmental significance.

5.2.2 Implications of Fe speciation in the Krycklan catchment

Iron speciation in soils and waters from the Krycklan catchment showed that Fe(II, III)-NOM complexes or Fe(II, III)-NOM complexes in combination with precipitated Fe(III) (hydr)oxides dominated Fe-speciation. These are in agreement with previous studies of Fe(III) model

systems[8,9] and other studies with natural soil and water samples[16,20,21,23]. However, Fe speciation is strongly affected by pH and these studies are mainly conducted at pH 3-7 which poses a limitation to the number of environments where these results could be directly applied. The occurrence of Fe(II, III)-NOM complexes over a wide range of pH values suggests that these complexes are important in organic rich environments[8]. As reported in Paper IV, at moderate loadings of Fe and Fe/As ratios, Fe(III)-NOM complexes make Fe(III) non-reactive towards As(V) which leads to elevated aqueous As(V) concentrations. This implies that natural, organic rich, environments containing even more species that may interact with Fe and/or NOM may contain elevated amounts of contaminants because of Fe(II, III)-NOM complexes.

5.3 The ternary As(V)/P(V)-Fe(III)-NOM systems

Despite the large scope of Paper IV (concentrations in the range 6485-67 243 ppm Fe, Fe/As ratios 0.5-100, pH 3-7 and use of multiple techniques) and the observed trends with respect to the interplay between Fe(III)-NOM complexes, $FeAsO_4$(s) and Fe(III)(hydr)oxides, there are still many gaps to be covered. The combined spectroscopic and modelling approach in this thesis highlighted the strong concentration dependence in the ternary systems. In the presence of NOM, concentrations of non-precipitated Fe(III) and As(V) species increases. Spectral interference complicated the WT analysis and the shell-by-shell EXAFS data fitting. Furthermore, in accordance with Paper IV, P-XANES may provide information regarding P speciation at larger Fe/P ratios that may be of higher environmental relevance compared with those present in Paper V.

5.3.1 Properties of Fe(III)-NOM complexes

The properties of NOM enable formation of stable Fe(III)-NOM complexes which exert pronounced effects on many geochemical cycles. Still, the properties of these Fe(III)-NOM complexes are not very well characterized. IR studies have indicated carboxylate groups as being important for complex formation at pH 3-7[9], but the high occurrence of other functional groups in NOM suggests that there may be other groups involved, especially at higher pH. The simple models presented in Papers IV and V only included 2 Fe(III)-NOM complexes for SRFA and SRN, respectively. Combined IR and potentiometric titrations at different Fe concentrations, similar to the Ga(III)-NOM study[8,9], may provide information regarding the number and properties of Fe(III)-NOM complexes.

The strength of the Fe(III)-NOM complexes is indicated to be quite high, as these complexes are observed over a large pH and Fe concentration interval. These could be more accurately determined if complementary, step-wise sample series were designed, i.e. an initial sample series where the acid/base properties of the organic material is determined, which is followed by a second sample series where Fe is added to the system at various total concentrations and pH-values, and a final series where As(V) is added under varying conditions. These sample series could, for instance, be analyzed with respect to pH, dissolved Fe(III) and As(V) concentrations, and concentrations of Fe(II) and As(III) that might have evolved from redox reactions. In order to obtain accurate thermodynamic models for the solid phases, subsystems not including the NOM have a high potential of being fruitful. The same discussion holds for Paper V, where As(V) is exchanged for P(V), which was even more difficult to assess via our EXAFS and IR spectroscopy approaches.

5.3.2 The identity of As(V)/P(V) bearing Fe phases

The collective results from Papers III-V indicate that speciation in the ternary As(V)/P(V)-Fe(III)-NOM systems is dominated by aqueous As(V)/P(V), Fe(III)-NOM complexes, $FeAsO_4(s)$, $FePO_4(s)$, $Fe(OH)_{1.5}(AsO_4)_{0.5}(s)$, $Fe(OH)_{1.5}(PO_4)_{0.5}(s)$ and $Fe(OH)_3(s)$. These results were obtained via a combination of IR and EXAFS spectroscopy and thermodynamic modelling. As(V) and P(V) adsorption to Fe minerals are well-established processes. Still, our data do not indicate these surface adsorbed species. Difficulties associated with the assignment of the element speciation include lack of soluble concentrations of Fe, As or P as these would help establish better models, lack of surface area and composition of solid phases, as well as the nature of XAS which only provides average CN and R, which may mask weak contributions. For a better understanding of environmentally relevant processes several key properties needs further characterization over a range of pH-values and Fe concentrations:

- Establish the effect of NOM on solid phase properties (size, surface area, and surface reactivity).
- Determine reactivity of solid phases formed in the presence of NOM towards selected elements, e.g. As(V) and P(V).

- Perform elemental characterization of solid phases formed in the presence of NOM, i.e. atomic ratios that might reveal the composition and extent of different solid phases, e.g. $Fe(OH)_3(s)$, $FeAsO_4(s)$ and mixed solid solutions where AsO_4^{3-} or PO_4^{3-} may be incorporated in the ferrihydrite bulk.
- Establish the effect of Fe/As or Fe/P ratios on the chemical composition of solid solutions in the presence of NOM.
- Identify the conditions (pH, concentrations, and Fe/As or Fe/P ratios) where surface adsorption and co-precipitation dominates, respectively.
- Determine the extent of stabilization of ferrihydrite, formed in the presence of NOM, induced by adsorption of As(V) or P(V)[118].

Our results indicate $FeAsO_4(s)$, $FePO_4(s)$ and the solid solutions ($Fe(OH)_{1.5}(AsO_4)_{0.5}(s)$, $Fe(OH)_{1.5}(PO_4)_{0.5}(s)$) to be more insoluble than ferrihydrite (Papers IV and V). Therefore, based on the stability of the solid phases, surface adsorbed species should be more mobile compared with co-precipitated species. Construction of refined models based on new data according to the list above may establish the mobility differences depending on dominating process (adsorption or co-precipitation).

Finally, do the ternary As(V)-Fe(III)-NOM complexes exist? No spectroscopic evidence for their existence was found in Paper III or IV, not even at high Fe(III) to As(V) ratios, e.g. ratios of 10-100 that have previously been reported as conditions where these complexes are formed. The lack of spectroscopic evidence does not mean that they do not exist, but we have not been able to probe them. Our results suggest that Fe(III) complexation via NOM protects Fe(III) from interactions with As(V) or P(V). Furthermore, the high occurrence of $FeAsO_4(s)$ (and $FePO_4(s)$) indicates the importance of (co)precipitation as another process limiting or suppressing the formation of ternary complexes.

6. Acknowledgement

I would like to acknowledge the funding agencies that have contributed to the work presented within this thesis: the faculty of science and technology at Umeå University, Formas (ForWater), Future Forest, the Kempe Foundation, Knut and Alice Wallenberg Foundation, Max-lab, SKB, the Swedish research council and SSRL. I would also like to acknowledge Wallenberg foundation, Kempe foundation, and Ångpanneföreningens forskningsstiftelse for travel grants to conferences.

Per, some eventful years have passed since I joined your group. I have learnt a lot from you and I am truly grateful that you gave me the opportunity be involved in a lot of interesting projects. Thank you for everything, especially the intense work lately. Staffan, more than seven years have passed since I sent you an e-mail inquiring about possible Bachelor thesis projects. You're a brilliant source of inspiration, knowledge, wisdom and kindness. It was great that we could get you involved in the ternary systems. I have also benefitted from great support from Torbjörn. Thanks for giving me hours and hours of discussions, for patiently answering my questions and for support, especially during last weeks before printing my thesis. Mats, my third assistant supervisor, thanks for your advice, feedback and sometimes, well-funded, skeptical questions.

Hjalmar has been another source of inspiration over the last couple of years. Thank you for always being so optimistic and encouraging and bringing and sharing good ideas. Your input has been very valuable. Thanks to Ida and Peder for all the help with and around the field work. It's been a pleasure to interact with you; everything has been smooth and easy, with a friendly tone and excellent performance.

I am also grateful for having met a lot of other special persons from the "good old days", with former inorganic chemistry and present members of our corridor and accompanying friends. Your company has made my time as a PhD-student much more pleasant. Thanks for being there in good times and in bad times. To Eva, thank you for the years of fruitful

friendship. I have enjoyed our work in the PhD council, in the committee for third cycle studies and our numerous chats over lunches and coffee breaks. Janice, thanks a lot for all your help and support with presentations, proofreading, various science and non-science related topics, for sharing your stories and making our group more alive. I will miss you a lot when you leave. Thanks to Anna and Jean-Francois for being my committee members, sharing your experience and providing advice. Jean-Francois is also acknowledged for proofreading parts of the kappa. Dan, Nils and Uwe are acknowledged for helping me to characterize my quite amorphous samples using X-ray diffraction. Thanks to Erik for help with the ICP-MS, it made Paper III feasible.

All my “outside of work friends” also deserves a big thank you, especially Erik, Katja and Ellen. Thanks for always being there. I have enjoyed our fikas, dinners, occasional excursions and sharing of everyday life. I would also like to take the opportunity to thank my parents, grandparents and parents in law for supporting my choices in life. Thanks for all the help and happy moments. Finally, Ola and Hampus, my two dearest ones, thanks for bringing perspectives and for making my life richer.

7. References

1. Borch, T.; Kretzschmar, R.; Kappler, A.; van Cappellen, P.; Ginder-Vogel, M.; Voegelin, A.; Campbell, K.: Biogeochemical redox processes and their impact on contaminant dynamics. *Environ. Sci. Technol.* **2010**, *44*, 15-23.
2. Cornell, R. M.; Schwertmann, U.: The iron oxides: structure, properties, reactions, occurrences and uses. *Wiley-VCH: Weinheim* **2003**.
3. Cismasu, A. C.; Michel, F. M.; Tcaciuc, A. P.; Tyliszczak, T.; Brown, J. G. E.: Composition and structural aspects of naturally occurring ferrihydrite. *C. R. Geosci.* **2011**, *343*, 210-218.
4. Mikutta, C.: X-ray absorption spectroscopy study on the effect of hydroxybenzoic acids on the formation and structure of ferrihydrite. *Geochim. Cosmochim. Acta* **2011**, *75*, 5122-5139.
5. Mikutta, C.; Frommer, J.; Voegelin, A.; Kaegi, R.; Kretzschmar, R.: Effect of citrate on the local Fe coordination in ferrihydrite, arsenate binding, and ternary arsenate complex formation. *Geochim. Cosmochim. Acta* **2010**, *74*, 5574-5592.
6. Amstaetter, K.; Borch, T.; Kappler, A.: Influence of humic acid imposed changes of ferrihydrite aggregation on microbial Fe(III) reduction. *Geochim. Cosmochim. Acta* **2012**, *85*, 326-341.
7. Shimizu, M.; Zhou, J.; Schröder, C.; Obst, M.; Kappler, A.; Borch, T.: Dissimilatory Reduction and Transformation of Ferrihydrite-Humic Acid Coprecipitates. *Environ. Sci. Technol.* **2013**, *47*, 13375-13384.
8. Karlsson, T.; Persson, P.: Coordination chemistry and hydrolysis of Fe(III) in a peat humic acid studied by X-ray absorption spectroscopy. *Geochim. Cosmochim. Acta* **2010**, *74*, 30-40.
9. Karlsson, T.; Persson, P.: Complexes with aquatic organic matter supress hydrolysis and precipitation of Fe(III). *Chem. Geol.* **2012**, *322–323*, 19-27.
10. Wang, S.; Mulligan, C.: Effect of natural organic matter on arsenic release from soils and sediments into groundwater. *Environ. Geoch. Health* **2006**, *28*, 197-214.
11. Stevenson, F. J.: Humus chemistry: genesis, composition, reactions. *New York, Wiley-Inter-science* **1982**.
12. Sposito, G.: The surface chemistry of soils. *UK: Oxford University press* **1984**.
13. Essington, M. E.: Soil and water chemistry: An integrative approach. *CRC Press LLC* **2004**.
14. Ritchie, J. D.; Perdue, E. M.: Proton-binding study of standard and reference fulvic acids, humic acids, and natural organic matter. *Geochim. Cosmochim. Acta* **2003**, *67*, 85-96.
15. Perdue, E. M.; Beck, K. C.; Helmut Reuter, J.: Organic complexes of iron and aluminium in natural waters. *Nature* **1976**, *260*, 418-420.

16. Karlsson, T.; Persson, P.; Skyllberg, U.; Mörth, C. M.; Giesler, R.: Characterization of iron(III) in organic soils using extended X-ray absorption fine structure spectroscopy. *Environ. Sci. Technol.* **2008**, *42*, 5449-5454.
17. Allard, T.; Menguy, N.; Salomon, J.; Calligaro, T.; Weber, T.; Calas, G.; Benedetti, M. F.: Revealing forms of iron in river-borne material from major tropical rivers of the Amazon Basin (Brazil). *Geochim. Cosmochim. Acta* **2004**, *68*, 3079-3094.
18. Ilina, S. M.; Poitrasson, F.; Lapitskiy, S. A.; Alekhin, Y. V.; Viers, J.; Pokrovsky, O. S.: Extreme iron isotope fractionation between colloids and particles of boreal and temperate organic-rich waters. *Geochim. Cosmochim. Acta* **2013**, *101*, 96-111.
19. Ingri, J.; Malinovsky, D.; Rodushkin, I.; Baxter, D. C.; Widerlund, A.; Andersson, P.; Gustafsson, Ö.; Forsling, W.; Öhlander, B.: Iron isotope fractionation in river colloidal matter. *Earth Planet. Sci. Lett.* **2006**, *245*, 792-798.
20. Neubauer, E.; Köhler, S. J.; von der Kammer, F.; Laudon, H.; Hofmann, T.: Effect of pH and Stream Order on Iron and Arsenic Speciation in Boreal Catchments. *Environ. Sci. Technol.* **2013**, *47*, 7120-7128.
21. Neubauer, E.; Schenkeveld, W. D. C.; Plathe, K. L.; Rentenberger, C.; von der Kammer, F.; Kraemer, S. M.; Hofmann, T.: The influence of pH on iron speciation in podzol extracts: Iron complexes with natural organic matter, and iron mineral nanoparticles. *Sci. Total Environ.* **2013**, *461–462*, 108-116.
22. Kleja, D. B.; van Schaik, J. W. J.; Persson, I.; Gustafsson, J. P.: Characterization of iron in floating surface films of some natural waters using EXAFS. *Chem. Geol.* **2012**, *326–327*, 19-26.
23. Sjöstedt, C.; Persson, I.; Hesterberg, D.; Kleja, D. B.; Borg, H.; Gustafsson, J. P.: Iron speciation in soft-water lakes and soils as determined by EXAFS spectroscopy and geochemical modelling. *Geochim. Cosmochim. Acta* **2013**, *105*, 172-186.
24. Viers, J.; Dupré, B.; Polvé, M.; Schott, J.; Dandurand, J.-L.; Braun, J.-J.: Chemical weathering in the drainage basin of a tropical watershed (Nsimi-Zoetele site, Cameroon) : comparison between organic-poor and organic-rich waters. *Chem. Geol.* **1997**, *140*, 181-206.
25. Prietzel, J.; Thieme, J.; Eusterhues, K.; Eichert, D.: Iron speciation in soils and soil aggregates by synchrotron-based X-ray microspectroscopy (XANES,μ-XANES). *Eur. J. Soil Sci.* **2007**, *58*, 1027-1041.
26. Rose, J.; Vilge, A.; Olivie-Lauquet, G.; Maison, A.; Frechou, C.; Bottero, J. Y.: Iron speciation in natural organic matter colloids. *Colloids Surf. A* **1998**, *136*, 11-19.
27. Emmenegger, L.; Schönenberger, R.; Sigg, L.; Sulzberger, B.: Light-induced redox cycling of iron in circumneutral lakes. *Limnol. Oceanogr.* **2001**, *46*, 49-61.
28. Lovley, D. R.: Microbial Fe(III) reduction in subsurface environments. *FEMS Microbiol. Rev.* **1997**, *20*, 305-313.

29. Pullin, M. J.; Cabaniss, S. E.: The effects of pH, ionic strength, and iron–fulvic acid interactions on the kinetics of non-photochemical iron transformations. I. Iron(II) oxidation and iron(III) colloid formation. *Geochim. Cosmochim. Acta* **2003**, *67*, 4067-4077.
30. Dos Santos Afonso, M.; Stumm, W.: Reductive dissolution of iron(III) (hydr)oxides by hydrogen sulfide. *Langmuir* **1992**, *8*, 1671-1675.
31. Smedley, P. L.; Kinniburgh, D. G.: A review of the source, behaviour and distribution of arsenic in natural waters. *Appl. Geochem.* **2002**, *17*, 517-568.
32. British Geological Survey, D.: Arsenic contamination of groundwater in Bangladesh. In: Kinniburgh D.G., Smedley P.L. (Eds.), British Geological Survey (Technical Report, WC/00/19.4 Volumes). *Brittish Geological Survey, Keyworth* **2001**.
33. WHO: Guidelines for drinking-water quality. Volume 1: Recommendations, 2nd ed. *WHO, Geneva* **2001**.
34. De Vitre, R.; Belzile, N.; Tessier, A.: Speciation and adsorption of arsenic on diagenetic iron oxyhydroxides. *Limnol. Oceanogr.* **1991**, *36*, 1480-1485.
35. Sullivan, K. A.; Aller, R. C.: Diagenetic cycling of arsenic in Amazon shelf sediments. *Geochim. Cosmochim. Acta* **1996**, *60*, 1465-1477.
36. Anderson, M. A.; Ferguson, J. F.; Gavis, J.: Arsenate adsorption on amorphous aluminum hydroxide. *J. Colloid Interface Sci.* **1976**, *54*, 391-399.
37. Ghosh, M. M.; Yuan, J. R.: Adsorption of inorganic arsenic and organoarsenicals on hydrous oxides. *Environ. Prog.* **1987**, *6*, 150-157.
38. Raven, K. P.; Jain, A.; Loeppert, R. H.: Arsenite and Arsenate Adsorption on Ferrihydrite: Kinetics, Equilibrium, and Adsorption Envelopes. *Environ. Sci. Technol.* **1998**, *32*, 344-349.
39. Pierce, M. L.; Moore, C. B.: Adsorption of arsenite and arsenate on amorphous iron hydroxide. *Water Res.* **1982**, *16*, 1247-1253.
40. Waychunas, G. A.; Fuller, C. C.; Rea, B. A.; Davis, J. A.: Wide angle X-ray scattering (WAXS) study of "two-line" ferrihydrite structure: Effect of arsenate sorption and counterion variation and comparison with EXAFS results. *Geochim. Cosmochim. Acta* **1996**, *60*, 1765-1781.
41. Wilkie, J. A.; Hering, J. G.: Adsorption of arsenic onto hydrous ferric oxide: effects of adsorbate/adsorbent ratios and co-occurring solutes. *Colloids Surf. A* **1996**, *107*, 97-110.
42. Jain, A.; Raven, K. P.; Loeppert, R. H.: Arsenite and Arsenate Adsorption on Ferrihydrite: Surface Charge Reduction and Net OH- Release Stoichiometry. *Environ. Sci. Technol.* **1999**, *33*, 1179-1184.
43. Manning, B. A.; Fendorf, S. E.; Goldberg, S.: Surface Structures and Stability of Arsenic(III) on Goethite: Spectroscopic Evidence for Inner-Sphere Complexes. *Environ. Sci. Technol.* **1998**, *32*, 2383-2388.
44. Fendorf, S.; Eick, M. J.; Grossl, P.; Sparks, D. L.: Arsenate and Chromate Retention Mechanisms on Goethite. 1. Surface Structure. *Environ. Sci. Technol.* **1997**, *31*, 315-320.

45. Hiemstra, T.; Van Riemsdijk, W. H.: A Surface Structural Approach to Ion Adsorption: The Charge Distribution (CD) Model. *J. Colloid Interface Sci.* **1996**, *179*, 488-508.
46. Loring, J. S.; Sandström, M. H.; Norén, K.; Persson, P.: Rethinking Arsenate Coordination at the Surface of Goethite. *Chem. Eur. J.* **2009**, *15*, 5063-5072.
47. Kocar, B. D.; Herbel, M. J.; Tufano, K. J.; Fendorf, S.: Contrasting Effects of Dissimilatory Iron(III) and Arsenic(V) Reduction on Arsenic Retention and Transport. *Environ. Sci. Technol.* **2006**, *40*, 6715-6721.
48. McArthur, J. M.; Banerjee, D. M.; Hudson-Edwards, K. A.; Mishra, R.; Purohit, R.; Ravenscroft, P.; Cronin, A.; Howarth, R. J.; Chatterjee, A.; Talukder, T.; Lowry, D.; Houghton, S.; Chadha, D. K.: Natural organic matter in sedimentary basins and its relation to arsenic in anoxic ground water: the example of West Bengal and its worldwide implications. *Appl. Geochem.* **2004**, *19*, 1255-1293.
49. McArthur, J. M.; Ravenscroft, P.; Safiulla, S.; Thirlwall, M. F.: Arsenic in groundwater: Testing pollution mechanisms for sedimentary aquifers in Bangladesh. *Water Resour. Res.* **2001**, *37*, 109-117.
50. Mladenov, N.; Zheng, Y.; Miller, M. P.; Nemergut, D. R.; Legg, T.; Simone, B.; Hageman, C.; Rahman, M. M.; Ahmed, K. M.; McKnight, D. M.: Dissolved Organic Matter Sources and Consequences for Iron and Arsenic Mobilization in Bangladesh Aquifers. *Environ. Sci. Technol.* **2009**, *44*, 123-128.
51. Ravenscroft, P.; McArthur, J. M.; Hoque, B. A.: Geochemical and palaeohydrological controls on pollution of groundwater by arsenic. In: Arsenic exposure and health effects IV. W.R. Chappell, C.O. Abernathy & R. Calderon (Eds). *Elsevier Science Ltd. Oxford* **2001**, 53-78.
52. Lagner, P.; Mikutta, C.; Kretzschmar, R.: Arsenic sequestration by organic sulphur in peat. *Nat. Geosci.* **2012**, *5*, 66-73.
53. Polizzotto, M. L.; Harvey, C. F.; Sutton, S. R.; Fendorf, S.: Processes conducive to the release and transport of arsenic into aqifers of Bangladesh. *Proc. Natl. Acad. Sci. U.S.A.* **2005**, *102*, 18819-18823.
54. Bauer, M.; Blodau, C.: Mobilization of arsenic by dissolved organic matter from iron oxides, soils and sediments. *Sci. Total Environ.* **2006**, *354*, 179-190.
55. Palmer, N. E.; Freudenthal, J. H.; von Wandruszka, R.: Reduction of Arsenates by Humic Materials. *Envir. Chem.* **2006**, *3*, 131-136.
56. Buschmann, J.; Kappeler, A.; Lindauer, U.; Kistler, D.; Berg, M.; Sigg, L.: Arsenite and Arsenate Binding to Dissolved Humic Acids: Influence of pH, Type of Humic Acid, and Aluminum. *Environ. Sci. Technol.* **2006**, *40*, 6015-6020.
57. Redman, A. D.; Macalady, D. L.; Ahmann, D.: Natural Organic Matter Affects Arsenic Speciation and Sorption onto Hematite. *Environ. Sci. Technol.* **2002**, *36*, 2889-2896.
58. Lin, H.-T.; Wang, M. C.; Li, G.-C.: Complexation of arsenate with humic substance in water extract of compost. *Chemosphere* **2004**, *56*, 1105-1112.

59. Mikutta, C.; Kretzschmar, R.: Spectroscopic evidence for ternary complex formation between arsenate and ferric iron complexes of humic substances. *Environ. Sci. Technol.* **2011**, *45*, 9550-9557.
60. Sharma, P.; Ofner, J.; Kappler, A.: Formation of Binary and Ternary Colloids and Dissolved Complexes of Organic Matter, Fe and As. *Environ. Sci. Technol.* **2010**, *44*, 4479-4485.
61. Hoffmann, M.; Mikutta, C.; Kretzschmar, R.: Arsenite Binding to Natural Organic Matter: Spectroscopic Evidence for Ligand Exchange and Ternary Complex Formation. *Environ. Sci. Technol.* **2013**, *47*, 12165-12173.
62. Dobran, S.; Zagury, G. J.: Arsenic speciation and mobilization in CCA-contaminated soils: Influence of organic matter content. *Sci. Total Environ.* **2006**, *364*, 239-250.
63. Ritter, K.; Aiken, G. R.; Ranville, J. F.; Bauer, M.; Macalady, D. L.: Evidence for the Aquatic Binding of Arsenate by Natural Organic Matter–Suspended Fe(III). *Environ. Sci. Technol.* **2006**, *40*, 5380-5387.
64. Rothwell, J. J.; Taylor, K. G.; Ander, E. L.; Evans, M. G.; Daniels, S. M.; Allott, T. E. H.: Arsenic retention and release in ombrotrophic peatlands. *Sci. Total Environ.* **2009**, *407*, 1405-1417.
65. González A, Z. I.; Krachler, M.; Cheburkin, A. K.; Shotyk, W.: Spatial Distribution of Natural Enrichments of Arsenic, Selenium, and Uranium in a Minerotrophic Peatland, Gola di Lago, Canton Ticino, Switzerland. *Environ. Sci. Technol.* **2006**, *40*, 6568-6574.
66. Brady, P. V.; House, W. A.: Surface-controlled dissolution and growth of minerals. In: Brady P.V., editor. Physics and chemistry of mineral surfaces, chap. 4. *London: CRC press* **1996**, 225-307.
67. Eveborn, D.; Gustafsson, J. P.; Hesterberg, D.; Hillier, S.: XANES Speciation of P in Environmental Samples: An Assessment of Filter Media for on-Site Wastewater Treatment. *Environ. Sci. Technol.* **2009**, *43*, 6515-6521.
68. Khare, N.; Hesterberg, D.; Martin, J. D.: XANES Investigation of Phosphate Sorption in Single and Binary Systems of Iron and Aluminum Oxide Minerals. *Environ. Sci. Technol.* **2005**, *39*, 2152-2160.
69. Meng, X.; Korfiatis, G. P.; Bang, S.; Bang, K. W.: Combined effects of anions on arsenic removal by iron hydroxides. *Toxicol. Lett.* **2002**, *133*, 103-111.
70. Meng, X.; Korfiatis, G. P.; Christodoulatos, C.; Bang, S.: Treatment of arsenic in Bangladesh well water using a household co-precipitation and filtration system. *Water Res.* **2001**, *35*, 2805-2810.
71. Geelhoed, J. S.; Hiemstra, T.; Van Riemsdijk, W. H.: Competitive Interaction between Phosphate and Citrate on Goethite. *Environ. Sci. Technol.* **1998**, *32*, 2119-2123.
72. Gu, B.; Schmitt, J.; Chen, Z.; Liang, L.; McCarthy, J. F.: Adsorption and desorption of natural organic matter on iron oxide: mechanisms and models. *Environ. Sci. Technol.* **1994**, *28*, 38-46.

73. Hawke, D.; Carpenter, P. D.; Hunter, K. A.: Competitive adsorption of phosphate on goethite in marine electrolytes. *Environ. Sci. Technol.* **1989**, *23*, 187-191.
74. Tipping, E.: The adsorption of aquatic humic substances by iron oxides. *Geochim. Cosmochim. Acta* **1981**, *45*, 191-199.
75. Newville, M.: Fundamentals of XAFS. *Consortium for Advanced Radiation Sources, University of Chicago, Chicago* **2004**.
76. Laudon, H.; Berggren, M.; Ågren, A.; Buffam, I.; Bishop, K.; Grabs, T.; Jansson, M.; Köhler, S.: Patterns and Dynamics of Dissolved Organic Carbon (DOC) in Boreal Streams: The Role of Processes, Connectivity, and Scaling. *Ecosystems* **2011**, *14*, 880-893.
77. Laudon, H.; Taberman, I.; Ågren, A.; Futter, M.; Ottosson-Löfvenius, M.; Bishop, K.: The Krycklan Catchment Study—A flagship infrastructure for hydrology, biogeochemistry, and climate research in the boreal landscape. *Water Resour. Res.* **2013**, *49*, 7154-7158.
78. Buffam, I.; Laudon, H.; Temnerud, J.; Mörth, C. M.; Bishop, K.: Landscape-scale variability of acidity and dissolved organic carbon during spring flood in a boreal stream network. *J. Geophys. Res.* **2007**, *112*, G01022.
79. Berggren, M.; Laudon, H.; Jansson, M.: Hydrological Control of Organic Carbon Support for Bacterial Growth in Boreal Headwater Streams. *Microb. Ecol.* **2009**, *57*, 170-178.
80. Ågren, A.; Buffam, I.; Jansson, M.; Laudon, H.: Importance of seasonality and small streams for the landscape regulation of dissolved organic carbon export. *J. Geophys. Res.* **2007**, *112*, G03003.
81. Björkvald, L.; Buffam, I.; Laudon, H.; Mörth, C. M.: Hydrogeochemistry of Fe and Mn in small boreal streams: The role of seasonality, landscape type and scale. *Geochim. Cosmochim. Acta* **2008**, *72*, 2789-2804.
82. Bishop, K.; Seibert, J.; Köhler, S.; Laudon, H.: Resolving the Double Paradox of rapidly mobilized old water with highly variable responses in runoff chemistry. *Hydrol. Process.* **2004**, *18*, 185-189.
83. Serkiz, S. M.; Perdue, E. M.: Isolation of dissolved organic matter from the suwannee river using reverse osmosis. *Water Res.* **1990**, *24*, 911-916.
84. Sun, L.; Perdue, E. M.; McCarthy, J. F.: Using reverse osmosis to obtain organic matter from surface and ground waters. *Water Res.* **1995**, *29*, 1471-1477.
85. Aiken, G. R.: "Isolation and concentration techniques for aquatic humic substances" in Aiken G.R., McKnight D.M., Wershaw R.L., MacCarthy P. (eds). Humic substances in soil, sediment and water: geochemistry and isolation. *Wiley-Interscience, New York* **1985**.
86. Thurman, E. M.; Malcolm, R. L.: Preparative isolation of aquatic humic substances. *Environ. Sci. Technol.* **1981**, *15*, 463-466.
87. Karlsson, M.; Lindgren, J.: WinSGW, a user interface for SolGasWater. *www.winsgw.se last visited February 3rd 2014* **2006**.

88. Eriksson, G.: An algorithm for the computation of aqueous multicomponent, multiphase equilibriums. *Anal. Chim. Acta* **1979**, *112*, 375-383.
89. Hagvall, K.; Persson, P.; Karlsson, T.: Spectroscopic characterization of the coordination chemistry and hydrolysis of gallium(III) in the presence of aquatic organic matter. *Manuscript submitted to Geochim. Cosmochim. Acta* **2014**.
90. Thibault, P.-J.; Rancourt, D. G.; Evans, R. J.; Dutrizac, J. E.: Mineralogical confirmation of a near-P:Fe=1:2 limiting stoichiometric ratio in colloidal P-bearing ferrihydrite-like hydrous ferric oxide. *Geochim. Cosmochim. Acta* **2009**, *73*, 364-376.
91. Bordas, F.; Bourg, A. C. M.: A critical evaluation of sample pretreatment of storage of contaminated sediments to be investigated for the potential mobility of their heavy metal load. *Water Air Soil Pollut.* **1998**, *103*, 137-149.
92. Rapin, F.; Tessier, A.; Campbell, P. G. C.; Carignan, R.: Potential artifacts in the determination of metal partitioning in sediments by sequential extraction procedure. *Environ. Sci. Technol.* **1986**, *20*, 836-840.
93. Thomson, E. A.; Luoma, S. N.; Cain, D. J.; Johansson, C.: The effect of sample storage on the extraction of Cu, Zn, Fe, Mn and organic material from oxidized estuarine sediment. *Water Air Soil Pollut.* **1980**, *14*, 215-233.
94. Bargar, J. R.; Persson, P.; Brown Jr, G. E.: Outer-sphere adsorption of Pb(II)EDTA on goethite. *Geochim. Cosmochim. Acta* **1999**, *63*, 2957-2969.
95. Kaplun, M.; Nordin, A.; Persson, P.: On the Anomalous Adsorption of [Pd(edta)]2- at the Water/Goethite Interface: Spectroscopic Evidence for Two Types of Surface Complexes. *Langmuir* **2007**, *24*, 483-489.
96. Ågren, A.; Buffam, I.; Berggren, M.; Bishop, K.; Jansson, M.; Laudon, H.: Dissolved organic carbon characteristics in boreal streams in a forest-wetland gradient during the transition between winter and summer. *J. Geophys. Res.* **2008**, *113*, G03031.
97. Wilke, M.; Farges, F.; Petit, P.-E.; Brown, J. G. E.; Martin, F.: Oxidation state and coordination of Fe in minerals: An Fe *K*-XANES spectroscopic study. *Am. Mineral.* **2001**, *86*, 714-730.
98. Funke, H.; Scheinost, A. C.; Chukalina, M.: Wavelet analysis of extended x-ray absorption fine structure data. *Phys. Rev. B* **2005**, *71*, 1-7.
99. Klementiev, K. V.: VIPER for Windows, freeware; K.V. Klementiev. *J. Phys. D: Appl. Phys.* **2001**, *34*, 209-217.
100. Webb, S. M.: SixPack: a graphical user interface for XAS analysis using IFEFFIT. *Phys. Scripta* **2005**, *T115*, 1011-1014.
101. Zabinsky, S. I.; Rehr, J. J.; Ankudinov, A.; Albers, R. C.; Eller, M. J.: Multiple scattering calculations of X-ray absorption spectra. *Phys. Rev. B* **1995**, *52*, 2995-3009.
102. Brigatti, M. F.; P., D.: Crystal-structure refinements of 1M plutonic biotites. *Am. Mineral.* **1990**, *75*, 305-313.

103. Szytuła, A.; Burewicz, A.; Dimitrijević, Ž.; Kraśnicki, S.; Rżany, H.; Todorović, J.; Wanic, A.; Wolski, W.: Neutron Diffraction Studies of α-FeOOH. *Phys. Status solidi (b)* **1968**, *26*, 429-434.
104. Kitahama, K.; Kiriyama, R.; Baba, Y.: Refinement of the crystal structure of scorodite. *Acta Cryst.* **1975**, *31*, 322-324.
105. Taxer, K.; Bartl, H.: On the dimorphy between the variscite and clinovariscite group: refined finestructural relationship of strengite and clinostrengite, $Fe(PO_4)\cdot 2H_2O$. *Cryst. Res. Technol.* **2004**, *39*, 1080-1088.
106. Persson, P.; Axe, K.: Adsorption of oxalate and malonate at the water-goethite interface: Molecular surface speciation from IR spectroscopy. *Geochim. Cosmochim. Acta* **2005**, *69*, 541-552.
107. Maillot, F.; Morin, G.; Wang, Y.; Bonnin, D.; Ildefonse, P.; Chaneac, C.; Calas, G.: New insight into the structure of nanocrystalline ferrihydrite: EXAFS evidence for tetrahedrally coordinated iron(III). *Geochim. Cosmochim. Acta* **2011**, *75*, 2708-2720.
108. Gustafsson, J. P.; Persson, I.; Kleja, D. B.; van Schaik, J. W. J.: Binding of Iron(III) to Organic Soils: EXAFS Spectroscopy and Chemical Equilibrium Modeling. *Environ. Sci. Technol.* **2007**, *41*, 1232-1237.
109. Manceau, A.: Critical evaluation of the revised akdalaite model for ferrihydrite. *Am. Mineral.* **2011**, *96*, 521-533.
110. Mikutta, C.; Mikutta, R.; Bonneville, S.; Wagner, F.; Voegelin, A.; Christl, I.; Kretzschmar, R.: Synthetic coprecipitates of exopolysaccharides and ferrihydrite. Part 1: Characterization. *Geochim. Cosmochim. Acta* **2008**, *72*, 1111-1127.
111. O'Day, P.; Rivera, J. N.; Root, R.; Carroll, S. A.: X-ray absorption spectroscopic study of Fe reference compounds for the analysis of natural sediments. *Am. Mineral.* **2004**, *89*, 572-585.
112. Fursova, E. Y.; Romanenko, G. V.; Ovcharenko, V. I.: Hexanuclear methanediolate-bridged iron(III) complex. *Russ. Chem. Bull.* **2005**, *54*, 811-813.
113. Manceau, A.; Matynia, A.: The nature of Cu bonding to natural organic matter. *Geochim. Cosmochim. Acta* **2010**, *74*, 2556-2580.
114. Sundman, A.; Karlsson, T.; Persson, P.: An Experimental Protocol for Structural Characterization of Fe in Dilute Natural Waters. *Environ. Sci. Technol.* **2013**, *47*, 8557-8564.
115. Sundman, A.; Karlsson, T.; Laudon, H.; Persson, P.: XAS study of iron speciation in soils and waters from a boreal catchment. *Chem. Geol.* **2014**, *364*, 93-102.
116. Edwards, D. C.; Myneni, S. C. B.: Hard and Soft X-ray Absorption Spectroscopic Investigation of Aqueous Fe(III)–Hydroxamate Siderophore Complexes. *J. Phys. Chem. A* **2005**, *109*, 10249-10256.
117. van Genuchten, C. M.; Addy, S. E. A.; Peña, J.; Gadgil, A. J.: Removing Arsenic from Synthetic Groundwater with Iron Electrocoagulation: An Fe and As K-Edge EXAFS Study. *Environ. Sci. Technol.* **2011**, *46*, 986-994.

118. Majzlan, J.: Thermodynamic Stabilization of Hydrous Ferric Oxide by Adsorption of Phosphate and Arsenate. *Environ. Sci. Technol.* **2011**, *45,* 4726-4732.